TRANSPARENT PROCESS OPEN ACCESS CHECK FOR UPDATES

Circadian rhythms of macrophages are altered by the acidic tumor microenvironment

Amelia M Knudsen-Clark [1], Daniel Mwangi [2], Juliana Cazarin [2], Kristina Morris[2], Cameron Baker [3], Lauren M Hablitz [4], Matthew N McCall[2,5,6], Minsoo Kim[1,6] & Brian J Altman [2,6] ✉

Abstract

Tumor-associated macrophages (TAMs) are prime therapeutic targets due to their pro-tumorigenic functions, but varying efficacy of macrophage-targeting therapies highlights our incomplete understanding of how macrophages are regulated within the tumor microenvironment (TME). The circadian clock is a key regulator of macrophage function, but how circadian rhythms of macrophages are influenced by the TME remains unknown. Here, we show that conditions associated with the TME such as polarizing stimuli, acidic pH, and lactate can alter circadian rhythms in macrophages. While cyclic AMP (cAMP) has been reported to play a role in macrophage response to acidic pH, our results indicate pH-driven changes in circadian rhythms are not mediated solely by cAMP signaling. Remarkably, circadian disorder of TAMs was revealed by clock correlation distance analysis. Our data suggest that hetero- geneity in circadian rhythms within the TAM population level may underlie this circadian disorder. Finally, we report that circadian regulation of macrophages suppresses tumor growth in a murine model of pancreatic cancer. Our work demonstrates a novel mechanism by which the TME influences macrophage biology through modulation of circadian rhythms.

Introduction

Tumor-associated macrophages (TAMs) are one of the most abundant leukocytes found in solid tumors, with high intra-tumoral TAM density generally associated with poor clinical outcome (Cassetta and Pollard, 2018; Gentles et al, 2015; Zhang et al, 2012). This is consistent with the largely pro-tumorigenic role

of macrophages within tumors (DeNardo and Ruffell, 2019). Macrophages are highly plastic professional phagocytes whose ability to sense and respond to the environment makes them uniquely equipped to protect tissue integrity under normal homeostatic conditions (Mosser and Edwards, 2008; Murray and Wynn, 2011). However, within the chronically inflamed tumor microenvironment (TME), failure to resolve the inflammation can lead to uncontrolled secretion of tissue repair factors by TAMs, promoting tumor growth and metastatic capacity (Coussens and Werb, 2002; Murray, 2018; Schoppmann et al, 2002). At the same time, conditions in the TME can drive TAMs to suppress potentially anti-tumorigenic inflammatory activity through various mechanisms including secretion of anti-inflammatory cytokines and expression of checkpoint inhibitors such as PD-L1, promoting immune suppression (Cook et al, 2013; DeNardo and Ruffell, 2019; Fadok et al, 1998; Graham et al, 2014; Huber et al, 2016b; Kuang et al, 2009; Roberts et al, 2017; Strassmann et al, 1994).

TAMs are known to suppress the response to many standard of care treatments through their pro-tumorigenic and immunosup-pressive functions, making them a prime therapeutic target (Ruffell and Coussens, 2015). However, we still have an incomplete understanding of how the TME influences macrophages, limiting our ability to target them; this is highlighted by the varying efficacy of therapeutic approaches used to target macrophages (Mantovani et al, 2022). This is thought to be due in part to the significant phenotypic heterogeneity of TAMs within tumors (Chevrier et al, 2017; Cuccarese et al, 2017; Mantovani et al, 2022). Evidence suggests this heterogeneity is due to the ability of macrophages to sense and adapt to the local microenvironment, which varies within tumors depending on several factors including the distance from blood vessels and neighboring cells (Huang et al, 2019; Laviron et al, 2022; Nalio Ramos et al, 2022; Yano et al, 2014). Indeed, various conditions in the TME have been shown to influence macrophage phenotype and function (DeNardo and Ruffell, 2019).

In particular, poor vascularization of solid tumors leads to inefficient delivery of oxygen, creating regions of hypoxia (Lyssiotis and Kimmelman, 2017). The hypoxic response promotes enhanced glycolytic activity of cells within the region, which, coupled with poor tissue drainage as a result of leaky vasculature, results in elevated levels of protons and lactate, acidifying the

---

[1]Department of Microbiology and Immunology, University of Rochester Medical Center, Rochester, NY, USA. [2]Department of Biomedical Genetics, University of Rochester Medical Center, Rochester, NY, USA. [3]Genomics Research Center, University of Rochester Medical Center, Rochester, NY, USA. [4]Center for Translational Neuromedicine, University of Rochester Medical Center, Rochester, NY, USA. [5]Department of Biostatistics and Computational Biology, University of Rochester Medical Center, Rochester, NY, USA. [6]Wilmot Cancer Institute, University of Rochester Medical Center, Rochester, NY, USA. ✉E-mail: Brian_Altman@URMC.rochester.edu

microenvironment (Gillies et al, 2019; Raghunand et al, 2003). Of conditions in the TME, it has been well appreciated that acidic (low) pH can promote a pro-resolution macrophage phenotype, thereby contributing to the pro-tumorigenic and immunosuppressive functions of macrophages within tumors (Bohn et al, 2018; El-Kenawi et al, 2019; Jiang et al, 2021b).

The myriad ways in which the TME can impact regulation of macrophages remain to be fully elucidated. Circadian rhythms are a key regulatory system present in almost all cells of the body, and are an understudied facet of macrophage biology (Partch et al, 2014). Acidic pH is a condition commonly associated with the TME that has been shown to alter circadian rhythms in cell lines (Walton et al, 2018); however, whether pH influences circadian rhythms in macrophages remain unknown.

Circadian rhythms are 24-h rhythms that impart oscillations in the levels of circadian-regulated gene transcripts and proteins in a tissue- and cell-specific manner, resulting in time-of-day-dependent variation in many cellular processes (Mure et al, 2018; Zhang et al, 2014). The molecular clock, which we will refer to as the circadian clock, drives these rhythms in cells through a cell-autonomous transcription/translation feedback loop, which is controlled in part by the transcription factor BMAL1 (Partch et al, 2014). Circadian clocks are synchronized by signals sent out from the central circadian clock housed within the suprachiasmatic nucleus of the hypothalamus, which entrains circadian clocks to the time of day (Partch et al, 2014). This allows for the temporal coordination of cells in spatially distinct tissues, although how the local microenvironment influences circadian rhythms remains to be elucidated.

All leukocytes tested to date have functional circadian clocks (Adrover et al, 2019; Arjona and Sarkar, 2005; Baumann et al, 2013; Druzd et al, 2017; Haspel et al, 2020; Keller et al, 2009; Nguyen et al, 2013; Silver et al, 2012a). As such, nearly every arm of the immune response (both innate and adaptive) is subject to circadian regulation (Haspel et al, 2020; Scheiermann et al, 2018; Silver et al, 2012a). Time-of-day-dependent regulation of immune responses is achieved through temporal gating of response to stimuli, effector function, and cell trafficking (Druzd et al, 2017; Fortier et al, 2011; Gibbs et al, 2012; He et al, 2018; Kitchen et al, 2020; Nobis et al, 2019), all of which promote coordination between the multiple phases of the immune response (Adrover et al, 2019; Beam et al, 2020; Druzd et al, 2017; Long et al, 2016; Mazzoccoli et al, 2011; Phillips et al, 2008; Silver et al, 2012b).

Key aspects of macrophage function are subject to circadian regulation, including cytokine secretion and phagocytosis (Curtis et al, 2015; Gibbs et al, 2012; Keller et al, 2009; Kitchen et al, 2020; Silver et al, 2012b). This results in a time-of-day-dependent macrophage response to stimuli, which modulates the magnitude of the resulting adaptive immune response and determines disease progression (Deng et al, 2018; Kitchen et al, 2020; Silver et al, 2012b). Circadian regulation of macrophages is of particular interest given recent evidence of 24-h circadian variation in the frequency of TAMs expressing surface markers associated with pro- or anti-tumorigenic phenotypes (Aiello et al, 2020; Strauss et al, 2020; Tsuruta et al, 2022). A promising application of such circadian variation was to leverage observations of circadian frequency in TAMs expressing immune checkpoint blockade (ICB) target PD-1 to subsequently increase efficacy of PD-1/PD-L1 ICB therapy by timing treatment to the time of day when PD-

1+ TAMs were most frequent (Qian et al, 2021; Tsuruta et al, 2022). This suggests that leveraging time-of-day variations in therapeutic targets could be a promising avenue to increase efficacy, highlighting the importance of understanding how circadian rhythms of macrophages may be influenced by conditions in the TME, which remains unclear.

In this work, we present evidence that circadian rhythms of macrophages are altered in the TME. We uncover a novel way in which two conditions within the TME, acidic pH and lactate, can influence macrophage biology through modulation of circadian rhythms. We also find that macrophages of different phenotypes have distinct circadian rhythms. Remarkably, we found evidence of circadian disorder in tumor-associated macrophages, indicating that circadian rhythms are altered in macrophages within the TME. Furthermore, our data suggest that heterogeneity in circadian rhythms at the population level may underlie the observed circadian disorder. This work elucidates a novel way in which the TME can alter macrophage biology, and represents the first steps to understanding how the tumor microenvironment can alter circadian rhythms of immune cells such as macrophages.

Results

Macrophages of different phenotypes exhibit different circadian rhythms

As macrophages are a phenotypically heterogeneous population in the TME, we first sought to understand whether diversity in macrophage phenotype could translate to diversity in circadian rhythms of macrophages. To this end, we used two well-established in vitro polarization models to study distinct macrophage phenotypes (Biswas and Mantovani, 2010; Mosser and Edwards, 2008; Munder et al, 1998; Murray, 2017; Viola et al, 2019). For a model of pro-inflammatory macrophages, we stimulated macrophages with interferon gamma (IFNγ) and lipopolysaccharide (LPS) to elicit a pro-inflammatory phenotype (Munder et al, 1998; Nathan et al, 1983). These macrophages are often referred to as 'M1' and are broadly viewed as anti-tumorigenic, and we will refer to them throughout this paper as 'pro-inflammatory' macrophages (Hörhold et al, 2020; Mills et al, 2000). For a model at the opposite end of the phenotypic spectrum, we stimulated macrophages with IL-4 and IL-13 (Munder et al, 1998; Stein et al, 1992). While these type 2 stimuli play a role in response to parasites and allergy, they are also major drivers of wound healing; in line with this, IL-4 and IL-13-stimulated macrophages have been well-characterized to adopt gene expression profiles associated with wound-healing and anti-inflammatory macrophage phenotypes (Allen, 2023; Mantovani et al, 2013; McWhorter et al, 2013; Pesce et al, 2009). As such, these macrophages are often used as a model to study pro-tumorigenic macrophages in vitro and are often referred to as 'M2' macrophages; throughout this paper, we will refer to IL-4 and IL-13-stimulated macrophages as 'pro-resolution' macrophages (Biswas et al, 2006; Ding et al, 2019; Mills et al, 2000). Consistent with previous studies, we found that genes associated with anti-inflammatory and pro-resolution programming characteristic of IL-4 and IL-13-stimulated macrophages such as *Arg1, Retnla, Chil3* (Ym1), *Clec10a* (MGL1), and *Mrc1* (CD206) were induced in IL-4 and IL-13-stimulated macrophages, but not IFNγ and
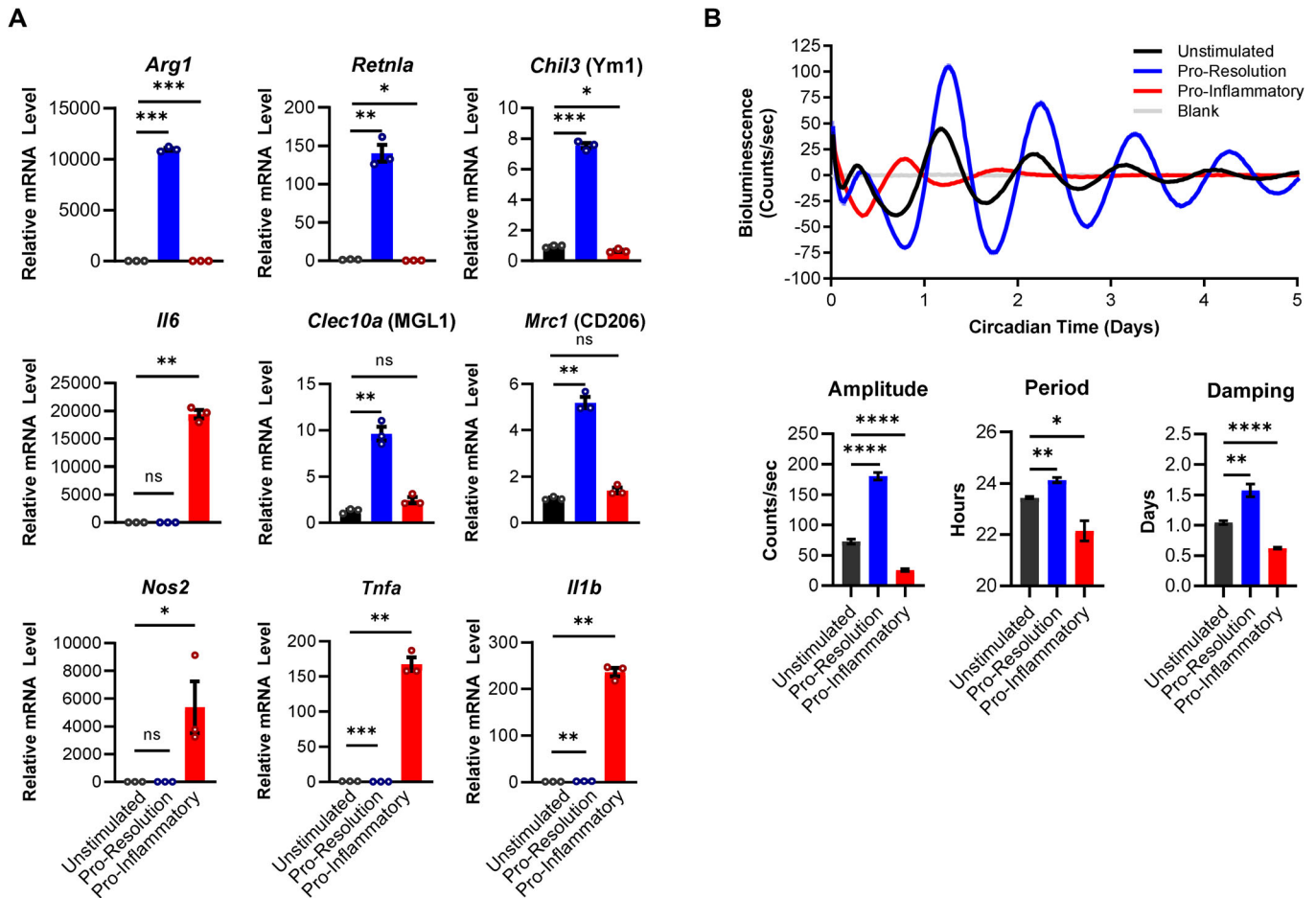
A

B

Figure 1. Macrophages of different phenotypes have distinct circadian rhythms.

Bone marrow-derived macrophages (BMDMs) were obtained from C57BL/6 mice expressing PER2-Luc. The circadian clocks of BMDMs were synchronized by a 24-h period of serum starvation in media with 0% serum, followed by a 2-h period of serum shock in media with 50% serum. BMDMs were then stimulated with either 10 ng/mL IL-4 and 10 ng/mL IL-13 (pro-resolution), or 50 ng/mL IFNγ and 100 ng/mL LPS (pro-inflammatory); or left unstimulated. (A) RNA was collected at 6 h post-synchronization, and qt-PCR was performed to assess expression of phenotype-associated genes. Shown are mean and standard error of the mean (SEM), $n = 3$ biological replicates. (B) Luciferase activity of BMDMs was monitored in real time by LumiCycle. Data was baseline-subtracted using the running average. Oscillation parameters of BMDMs were measured by LumiCycle Analysis. Shown are mean and standard error of the mean (SEM), $n = 5$ biological replicates. Data information: Statistical significance was determined by unpaired two-tailed t-test with Welch's correction of unstimulated vs pro-inflammatory or unstimulated vs pro-resolution; *$p < 0.05$; **$p < 0.005$; ***$p < 0.0005$; ****$p < 0.0001$; ns: not significant. Experiment was replicated twice. Exact p values: (A) *Arg1* 0.0002 (unstimulated vs pro-resolution), 0.0005 (unstimulated vs pro-inflammatory); *Retnla* 0.0061 (unstimulated vs pro-resolution), 0.0387 (unstimulated vs pro-inflammatory); *Chil3* 0.0003 (unstimulated vs pro-resolution), 0.0278 (unstimulated vs pro-inflammatory); *Il6* 0.0016 (unstimulated vs pro-inflammatory); *Clec10a* 0.0062 (unstimulated vs pro-resolution); *Mrc1* 0.0026 (unstimulated vs pro-resolution); *Nos2* 0.0462 (unstimulated vs pro-inflammatory); *Tnfa* 0.0006 (unstimulated vs pro-resolution), 0.0034 (unstimulated vs pro-inflammatory); *Il1b* 0.0029 (unstimulated vs pro-resolution), 0.0016 (unstimulated vs pro-inflammatory). (B) Amplitude <0.0001 (unstimulated vs pro-resolution), <0.0001 (unstimulated vs pro-inflammatory); Period 0.0018 (unstimulated vs pro-resolution), 0.0299 (unstimulated vs pro-inflammatory); Damping 0.0059 (unstimulated vs pro-resolution), <0.0001 (unstimulated vs pro-inflammatory).

LPS-stimulated macrophages. In contrast, genes associated with pro-inflammatory activity characteristic of IFNγ and LPS-stimulated macrophages such as *Nos2* (iNOS), *Tnfa, Il1b,* and *Il6* were induced in IFNγ and LPS-stimulated macrophages, but not IL-4 and IL-13-stimulated macrophages (Fig. 1A) (Binger et al, 2015; El-Kenawi et al, 2019; Hörhold et al, 2020; Jiang et al, 2021b; Martinez and Gordon, 2014; McWhorter et al, 2013). This indicates that macrophages stimulated with IL-4 and IL-13 were polarized toward a pro-resolution phenotype, while macrophages stimulated with IFNγ and LPS were polarized toward a pro-inflammatory phenotype.

Circadian rhythms of macrophages were measured by monitoring PER2, a key component of the circadian clock, via the rhythmic activity of the PER2-Luciferase (PER2-Luc) fusion protein in a live cell LumiCycle luminometer (Fig. EV1A) (Yoo et al, 2004). Bone marrow-derived macrophages (BMDMs) were generated from bone marrow of mice expressing PER2-Luc. Following differentiation, the circadian clocks of BMDMs were synchronized by a 24-h period of serum starvation followed by 2 h of serum shock (Collins et al, 2021), and rhythms were observed for up to 4 days (Fig. EV1B,C).

To determine whether phenotype can influence circadian rhythms in macrophages, BMDMs were cultured in the presence

or absence of polarizing stimuli, and rhythms were observed by LumiCycle (Fig. 1B). The amplitude of rhythms is the magnitude of change between the peak and the trough, and is indicative of the strength of rhythms (Rodheim et al, 2021; Wu et al, 2021). Amplitude of rhythms was suppressed in pro-inflammatory macrophages compared to unstimulated macrophages. In contrast, amplitude of rhythms in pro-resolution macrophages was enhanced. This suggests that rhythms are suppressed in pro-inflammatory macrophages but enhanced in pro-resolution macrophages, which agrees with previous observations (Chen et al, 2020; Lellupitiyage Don et al, 2022). Period is the amount of time it takes to complete one full oscillation (Pilorz et al, 2014). Compared to unstimulated macrophages, period was lengthened in pro-resolution macrophages but shortened in pro-inflammatory macrophages. This is in line with others' observations and suggests that the clock runs with a longer period (slower) in pro-resolution macrophages but runs with a shorter period (faster) in pro-inflammatory macrophages (Chen et al, 2020; Lellupitiyage Don et al, 2022).

Interestingly, we observed differences in damping of rhythms in polarized macrophages. Damping is measured as the number of days required for the amplitude of rhythms to decrease by 30% of the first cycle (Abe et al, 2002). Damping of rhythms in most free-running cell populations (defined as cells cultured in the absence of external synchronizing stimuli) occurs naturally as the circadian clocks of individual cells in the population become desynchronized from each other; thus, damping can be indicative of desynchrony within a population (Gaspar et al, 2019). The damping rate increases as the time it takes for rhythms to dissipate decreases; conversely, as damping rate decreases as the time it takes for rhythms to dissipate increases. We observed increased rate of damping in pro-inflammatory macrophages compared to unstimulated macrophages (Fig. 1B), indicating that population-level rhythms were maintained for a shorter length of time in pro-inflammatory macrophages. In contrast, damping rate was decreased in pro-resolution macrophages, indicating that population-level rhythms were maintained for longer in pro-resolution macrophages. These data suggest that pro-inflammatory macrophages may have an impaired ability to maintain synchrony, while pro-resolution macrophages may have an enhanced ability to maintain synchrony.

Collectively, these data suggest that pro-inflammatory macrophages have weaker rhythms and impaired ability to maintain synchrony, while pro-resolution macrophages have enhanced rhythms and an increased ability to maintain synchrony. This is evidence that macrophages of different phenotypes have distinct circadian rhythms, suggesting that diversity of macrophage phenotype may lead to diversity in macrophage circadian rhythms.

Acidic pH alters circadian rhythms of macrophages

The TME has previously been shown to be acidic, with a pH ranging from 6.8 to 6.3; much more acidic than the typical pH in blood and healthy tissue of 7.3–7.4 (Boedtkjer and Pedersen, 2020; Estrella et al, 2013; Gillies et al, 1994). It was previously reported that acidic pH can alter circadian rhythms in cell lines, but whether this applies to macrophages remains unknown (Walton et al, 2018). Thus, we cultured BMDMs under conditions of varying pH within a range that mimics that found within the TME (pH 6.5–7.4). As

macrophages are a heterogeneous population in the TME, we assessed the influence of acidic pH on rhythms of unstimulated, pro-resolution, and pro-inflammatory macrophages. In line with previous observations, macrophages cultured at pH 6.5 were polarized toward a pro-resolution phenotype, characterized by increased expression of Arg1 and Vegf compared to macrophages cultured at pH 7.4 (Fig. EV2A). Pro-inflammatory macrophages cultured at pH 6.5 had decreased expression of Nos2 compared to those cultured at pH 7.4, suggesting that an acidic pH of 6.5 both promotes a pro-resolution phenotype and suppresses a pro-inflammatory phenotype.

It has been observed that inducible cyclic AMP early repressor (Icer), an isoform of cyclic AMP (cAMP)-response modulator (Crem), is upregulated downstream of acid-sensing in macrophages, and has been used as a "biomarker" for macrophages exposed to acidic conditions in tumors. We observed induction of Icer in unstimulated and pro-resolution macrophages cultured at pH 6.5 compared to pH 7.4, indicating that these macrophages were sensing acidic conditions (Fig. EV2B). In line with previous observations that Icer is induced downstream of LPS-driven TLR4 signaling, Icer was also upregulated in pro-inflammatory macrophages compared to unstimulated macrophages even at neutral pH 7.4 (Lv et al, 2017). Although Icer was not further upregulated in pro-inflammatory macrophages at pH 6.5 compared to pH 7.4, Nos2 was suppressed at pH 6.5 compared to pH 7.4, suggesting that pro-inflammatory macrophages responded to acidic pH. In all, these data confirm that macrophages of various phenotypes can sense and respond to acidic conditions within the range of pH found in the TME.

To determine whether an acidic microenvironment influences circadian rhythms in macrophages, we assessed rhythms of unstimulated, pro-resolution, and pro-inflammatory macrophages under normal and acidic conditions. To this end, BMDMs were polarized toward a pro-resolution or a pro-inflammatory phenotype, or left unstimulated, and cultured in media at a normal pH of 7.4 or at acidic pH of 6.8 or 6.5; PER2-Luc rhythms were then observed by LumiCycle. In unstimulated and pro-resolution BMDMs, lower pH led to enhanced amplitude, a shortening in period, and increased damping rate of rhythms at pH 6.8 and pH 6.5 relative to neutral pH 7.4 (Fig. 2A,B; Appendix Fig. S1A). This suggests that in unstimulated and pro-resolution macrophages, acidic pH can strengthen rhythms by enhancing amplitude and speeding up the circadian clock, but may impair ability to maintain synchrony. Notably, changes in amplitude and period occurred in a dose-dependent fashion as pH decreased, indicating that rhythms are altered in a pH-dependent manner. In contrast, pro-inflammatory macrophages cultured at pH 6.5 exhibited suppressed amplitude, elongated period, and decreased damping rate of rhythms compared to those cultured at pH 7.4 (Fig. 2C; Appendix Fig. S1A). This suggests that in pro-inflammatory macrophages, acidic pH can weaken rhythms by decreasing amplitude and slowing down the speed of the clock, but may promote the ability to maintain synchrony. Low pH was also observed to alter the expression of the circadian clock genes Per2, Cry1, and Nr1d1 (REV-ERBα) over time across different macrophage phenotypes, confirming that multiple components of the circadian clock are altered by acidic pH (Fig. 2D–F; Appendix Fig. S1B). Notably, the patterns in expression of circadian genes did not always match the patterns of PER2-Luc levels observed by LumiCycle. This is perhaps
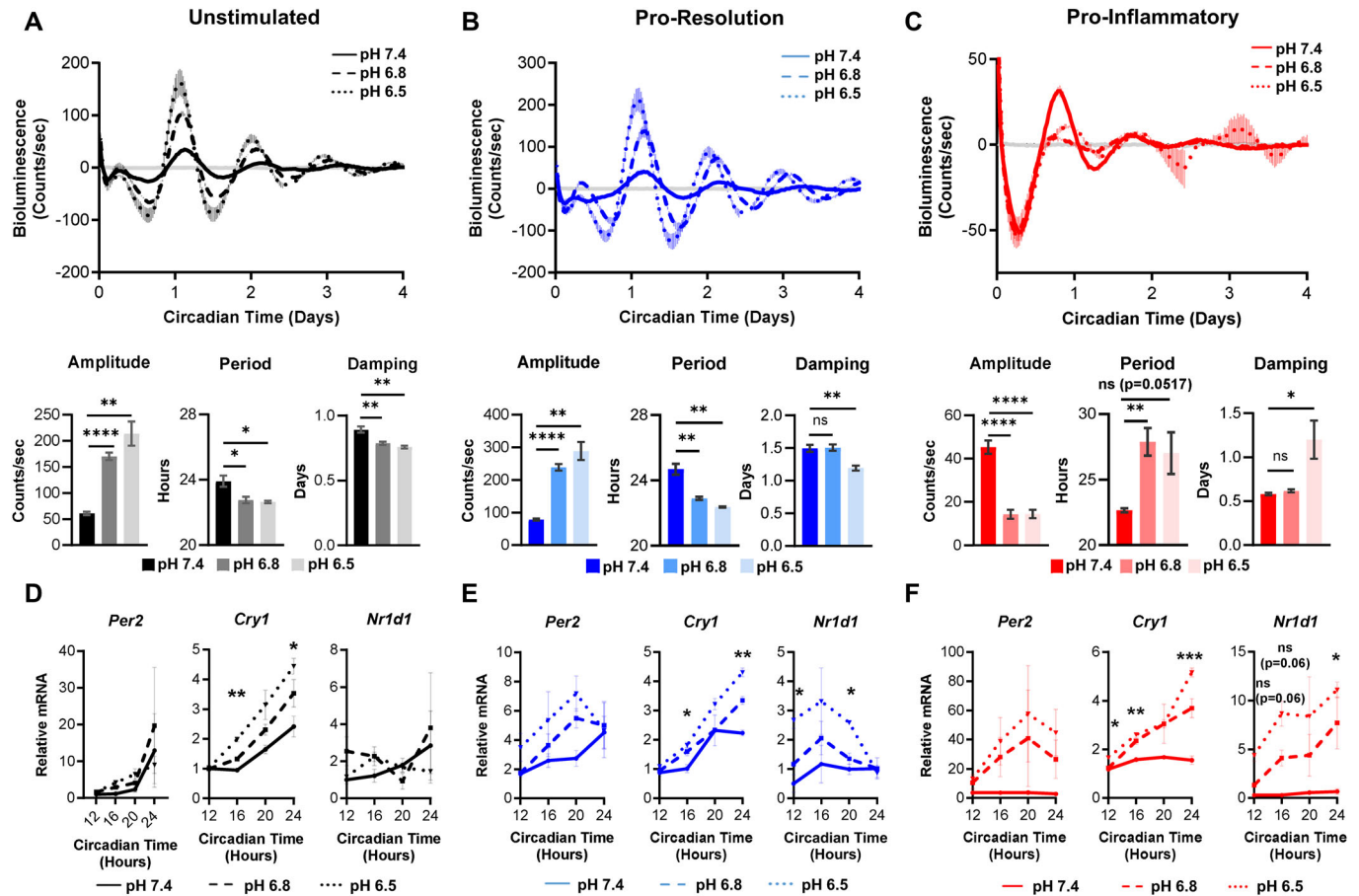
Figure 2. Acidic pH alters circadian rhythms of bone marrow-derived macrophages in vitro.

(A–F) Bone marrow-derived macrophages (BMDMs) were obtained from C57BL/6 mice expressing PER2-Luc. The circadian clocks of BMDMs were synchronized by a 24-h period of serum starvation in media with 0% serum, followed by a 2-h period of serum shock in media with 50% serum. BMDMs were then cultured in media with neutral pH 7.4 or acidic media with pH 6.8 or 6.5, and stimulated with either (B, E) 10 ng/mL IL-4 and 10 ng/mL IL-13 (pro-resolution), or (C, F) 50 ng/mL IFNγ and 100 ng/mL LPS (pro-inflammatory); or (A, D) left unstimulated. (A–C). Luciferase activity was monitored in real time by LumiCycle, n = 2 biological replicates. Data from both experiments was baseline-subtracted using the running average, and oscillation parameters were measured by LumiCycle Analysis, n = 5 biological replicates. (D–F). In parallel, RNA was collected at 12, 16, 20, and 24 h post-synchronization, and qt-PCR was performed to assess oscillation of transcripts encoding core clock proteins in macrophages under acidic conditions. n = 3 biological replicates. Data information: For (A–C), top panel (LumiCycle traces), shown are mean and SEM, experiment was replicated twice. For bottom panel (LumiCycle parameter analysis), shown are mean and SEM. For (D–F), shown are mean and SEM. Experiment was replicated twice. For all panels, statistical significance was determined by unpaired two-tailed t-test with Welch's correction of pH 7.4 vs pH 6.8 or 6.5 (pH 7.4 vs 6.8 was not tested in D–F). The Holm-Šídák correction for multiple t-tests was applied; *p < 0.05; **p < 0.005; ***p < 0.0005; ****p < 0.0001; ns: not significant. Exact p values: (A). Amplitude <0.0001 (pH 7.4 vs 6.8), 0.0025 (pH 7.4 vs 6.5); Period 0.0243 (pH 7.4 vs 6.8), 0.0184 (pH 7.4 vs 6.5); Damping 0.0098 (pH 7.4 vs 6.8), 0.0035 (pH 7.4 vs 6.5). (B) Amplitude <0.0001 (pH 7.4 vs 6.8), 0.0014 (pH 7.4 vs 6.5); Period 0.0039 (pH 7.4 vs 6.8), 0.002 (pH 7.4 vs 6.5); Damping 0.0022 (pH 7.4 vs 6.5). (C) Amplitude <0.0001 (pH 7.4 vs 6.8), <0.0001 (pH 7.4 vs 6.5); Period 0.0073 (pH 7.4 vs 6.8), 0.0517 (pH 7.4 vs 6.5); Damping 0.046 (pH 7.4 vs 6.5). (D) Cry1 0.005321 (pH 7.4 vs pH 6.5 CT 16), 0.03417 (pH 7.4 vs pH 6.5 CT 24). (E) Cry1 0035141 (pH 7.4 vs pH 6.5 CT 16), 0.002073 (pH 7.4 vs pH 6.5 CT 24); Nr1d1 0.025736 (pH 7.4 vs pH 6.5 CT 12), 0.036436 (pH 7.4 vs pH 6.5 CT 20). (F) Cry1 0.014339 (pH 7.4 vs pH 6.5 CT 12), 0.005812 (pH 7.4 vs pH 6.5 CT 16), 0.000525 (pH 7.4 vs pH 6.5 CT 24); Nr1d1 0.062514 (pH 7.4 vs pH 6.5 CT 12), 0.062514 (pH 7.4 vs pH 6.5 CT 16), 0.010905 (pH 7.4 vs pH 6.5 CT 24). Some 'ns' have been omitted from (D–F) for visual clarity.

unsurprising, as circadian rhythms are regulated at multiple levels (transcriptional, post-transcriptional, translational, post-translational); as a result, circadian patterns observed in circadian proteins such as PER2-Luc do not always match those of their gene transcripts (Collins et al, 2021). Together, these data indicate that exposure to acidic pH can induce changes in circadian rhythms of macrophages. Interestingly, our data indicate that while rhythms of unstimulated and pro-resolution macrophages are enhanced under acidic pH despite increased damping rate, rhythms of pro-inflammatory macrophages are suppressed under acidic conditions but have improved damping rate. This suggests that acidic pH

modulates rhythms differently in macrophage of different phenotypes.

The observation that acidic pH can enhance rhythms is particularly interesting, given that acidic pH is a stressful condition that can compromise macrophage survival (Appendix Fig. S2A) (Jiang et al, 2021b). In line with their documented enhanced glycolytic capacity, pro-inflammatory macrophages acidified the media over time (Appendix Fig. S2B). Notably, while pH of the media the pro-inflammatory macrophages were cultured in decreased over time pH, the pH differential between the pH 7.4, pH 6.8, and pH 6.5 samples groups of pro-inflammatory
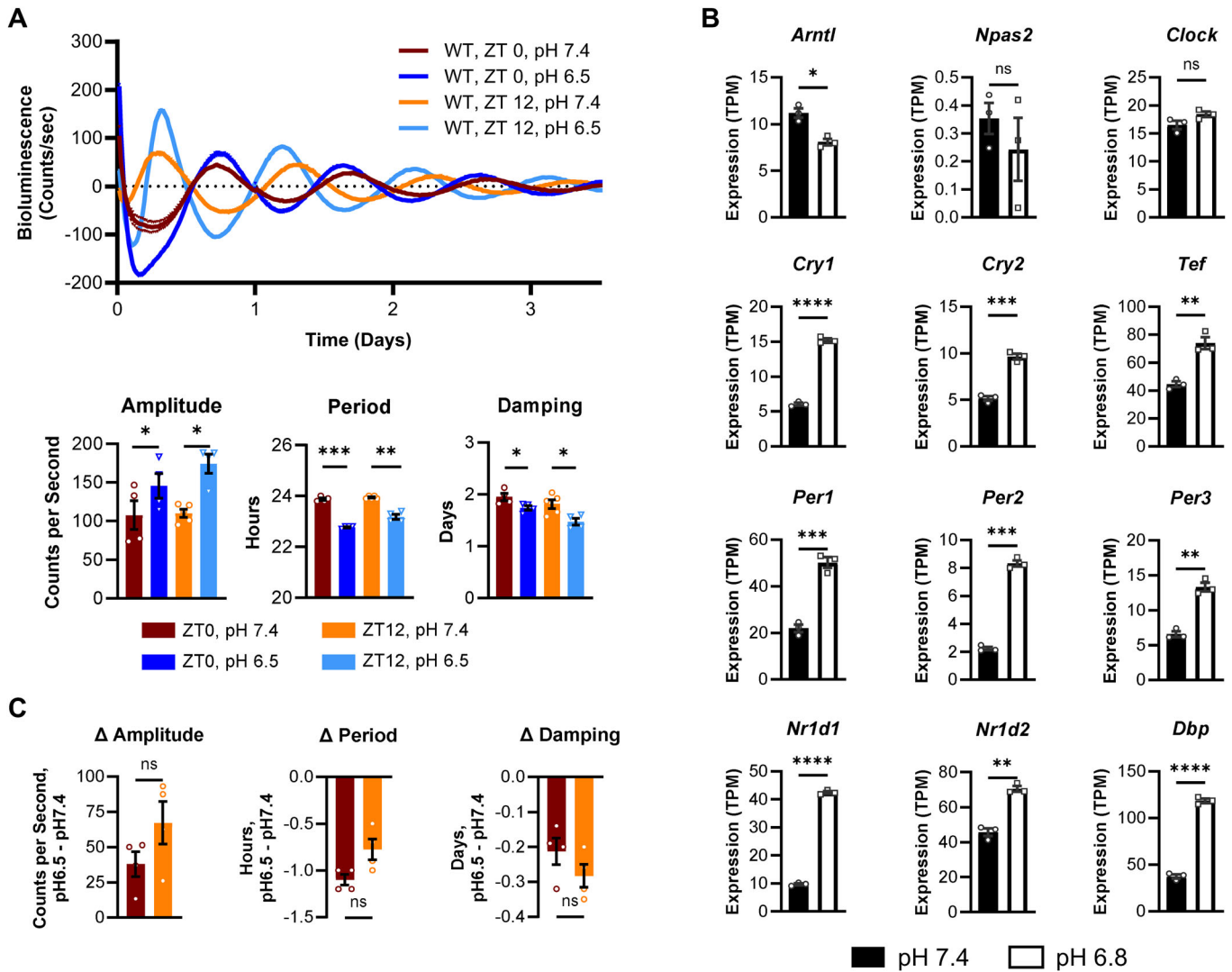
Figure 3. Acidic pH alters circadian rhythms of peritoneal macrophages ex vivo at temporally distinct times of day.

(A) Peritoneal macrophages were obtained at ZT0 or ZT12 from C57BL/6 mice expressing Per2-Luc and cultured in media with neutral pH 7.4 or acidic pH 6.5. (A) Luciferase activity was monitored in real time by LumiCycle. Data was baseline-subtracted using the running average; $n = 2$ biological replicates, each replicate and connecting line shown. Oscillation parameters were measured by LumiCycle Analysis; shown is the mean and SEM, $n = 4$ biological replicates, data pooled from 2 independent experiments. (B) Clock gene expression, in transcripts per million (TPM), of peritoneal macrophages cultured in media at pH 7.4 or pH 6.8 for 24 h, sourced from publicly available data (Data ref: GSE164697), $n = 3$ biological replicates [30]. (C) The magnitude of change in circadian oscillation parameters from (A) between macrophages at pH 7.4 and pH 6.5 was compared between peritoneal macrophages taken at ZT0 or ZT12. $n = 4$ biological replicates; data pooled from 2 independent experiments. Data information: For (A), shown are individual points and mean, experiment was replicated twice. For (B), shown is mean and SEM, For (C), shown is the mean and SEM experiment replicated twice. For all panels, statistical significance was determined by paired two-tailed t-test with Welch's correction; *$p < 0.05$; **$p < 0.005$; ***$p < 0.0005$; ns: not significant. Exact p values: (A) Amplitude 0.0231 (ZT0 pH 7.4 vs pH 6.5), 0.0204 (ZT12 pH 7.4 vs pH 6.5); Period 0.0003 (ZT0 pH 7.4 vs pH 6.5), 0.0043 (ZT12 pH 7.4 vs pH 6.5); Damping 0.0104 (ZT0 pH 7.4 vs pH 6.5), 0.0317 (ZT12 pH 7.4 vs pH 6.5). (B) *Arntl* 0.0103; *Cry1* < 0.0001; *Cry2* 0.0004; *Tef* 0.0093; *Per1* 0.0009; *Per2* 0.0001; *Per3* 0.0017; *Nr1d1* < 0.0001; *Nr1d2* 0.0012; *Dbp* < 0.0001.

macrophages was maintained out to 2 days, consistent with the changes in rhythms that we observe and measure between these groups.

While BMDMs are a widely used model for studying macrophages in vitro, there are biological differences between BMDMs generated in culture and tissue-resident macrophages. Thus, we sought to determine whether our observations of pH-induced changes in rhythms were relevant to tissue-resident macrophages

differentiated in vivo. To this end, we harvested peritoneal macrophages from mice expressing PER2-Luc either in the morning at ZT0 (6 AM) or in the evening at ZT12 (6 PM). Peritoneal macrophages were cultured in media at neutral pH of 7.4 or acidic pH of 6.5 and observed by LumiCycle. Recapitulating our results in BMDMs, peritoneal macrophages exhibited increased amplitude, decreased period, and increase rate of damping at pH 6.5 compared to pH 7.4 (Fig. 3A). To test whether pH-driven

changes in circadian rhythms of peritoneal macrophages were reflected at the mRNA level, we compared expression of circadian clock genes in peritoneal macrophages cultured at neutral pH 7.4 or acidic pH 6.8 for 24 h using publicly available RNA-sequencing data (Jiang et al, 2021b; Jiang et al, 2021a). In line with altered circadian rhythms observed by Lumicycle, peritoneal macrophages cultured at pH 6.8 expressed different levels of circadian clock genes than peritoneal macrophages culture at pH 7.4 (Fig. 3B). The trends in changes of gene expression in peritoneal macrophages cultured at pH 6.8 matched what we observed in BMDMs, where low pH generally led to higher levels of circadian clock gene expression (Fig. 2D–F). These data support our observations by LumiCycle and indicate that acidic pH drives transcriptional changes in multiple components of the circadian clock. In all, these data are evidence that pH-dependent changes in circadian rhythms are relevant to in vivo-differentiated macrophages.

Circadian rhythms confer time-of-day variability in response to stimuli. As we have observed that acidic pH can influence circadian rhythms of peritoneal macrophages, we sought to understand if peritoneal macrophages would be more or less susceptible to pH-induced changes in rhythms depending on time of day of exposure. To this end, we compared the magnitude of change in amplitude, period, and damping in peritoneal macrophages when exposed to acidic pH 6.5 compared to neutral pH 7.4 at different times of day (Fig. 3C). We observed no significant difference in the pH-driven change in amplitude, period, or damping in rhythms of peritoneal macrophages taken in the morning at ZT0 compared to those taken in the evening at ZT12. This indicates that the influence of pH on rhythms of macrophages was similar when exposed to acidic pH in the morning or in the evening, which suggests that macrophages are similarly susceptible to pH-induced changes in rhythms regardless of time of day of exposure.

Lactate alters circadian rhythms of macrophages in a manner distinct from acidic pH

Elevated lactate concentrations often co-localize to regions of high acidity, due to the export of both protons and lactate by glycolytic cells (Kraut and Madias, 2014; Pastorekova and Gillies, 2019; Swietach, 2019). In tumors, lactate has been observed in concentrations of up to 30 mM, which is elevated over typical lactate levels in blood and healthy tissue of 1.5–3 mM (de la Cruz-López et al, 2019). There are previous reports that lactic acid can promote polarization of macrophages toward a pro-resolution phenotype (Colegio et al, 2014). Thus, we sought to understand if lactate may be a feature of the TME capable of influencing circadian rhythms of macrophages, in addition to acidic pH. To this end, we cultured BMDMs in the presence or absence of 25 mM sodium-L-lactate. In line with previous observations, BMDMs exposed to lactate had elevated levels of Vegf; however, we did not observe significant elevation of Arg1 (Fig. 4A) (Colegio et al, 2014).

We next cultured BMDMs at normal pH 7.4 or acidic pH 6.5, in the presence or absence of 25 mM sodium-L-lactate, and monitored circadian rhythms (Fig. 4B,C; Appendix Fig. S3A). Rhythms of BMDMs at pH 7.4 exposed to lactate had an elongated period and decreased damping time compared to BMDMs cultured at pH 7.4 without lactate (Fig. 4B). This suggests that lactate can slow the circadian clock and may impair the ability of macrophages to

maintain synchrony. Interestingly, these changes in rhythms are different from those observed in acidic conditions, indicating that lactate can modulate circadian rhythms in macrophages in a manner distinct from acidic pH.

As previously observed, macrophages exposed to acidic pH 6.5 exhibited increased amplitude, shortened period, and increased damping rate of circadian rhythms. When BMDMs were exposed to both acidic pH and elevated lactate, the increased amplitude observed at pH 6.5 was maintained; however, the shortened period observed at pH 6.5 was lost, with period lengthened in BMDMs cultured in 25 mM sodium-l-lactate (Fig. 4B). The increased damping rate of rhythms in BMDMs cultured at pH 6.5 compared to pH 7.4 was maintained, and was further dampened by exposure to lactate (Fig. 4B). These data indicate that changes in rhythms associated with acidic conditions persisted when co-exposed to elevated lactate. Lactate was also observed to alter expression of the circadian clock genes Per2, Cry1, and Nr1d1 over time in BMDMs cultured at pH 6.5, while having more subtle effects at pH 7.4 (Fig. 4C). Notably, lactate blunted the effect of pH 6.5 on Cry1 expression, while enhancing the effect of low pH on Nr1d1 expression. In all, these data indicate that concentration of lactate similar to that present in the TME can influence circadian rhythms and circadian clock gene expression of macrophages. Lactate altered rhythms differently than acidic pH, and when macrophages were exposed to acidic pH and lactate together, rhythms were further altered. This suggests that when macrophages are exposed to multiple conditions capable of altering circadian rhythms, each condition may contribute to a combined effect on rhythms that differs from its individual impact.

Cancer cell supernatant alters circadian rhythms in macrophages in a manner partially reversed by neutralization of pH

We have observed that polarizing stimuli, acidic pH, and lactate can alter circadian rhythms. However, the tumor microenvironment is complex. Cancer cells secrete a variety of factors and deplete nutrients in the environment. To model this, we cultured BMDMs in RPMI or supernatant collected from KCKO cells, which are a murine model of pancreatic ductal adenocarcinoma (PDAC) (Besmer et al, 2011; Kidiyoor et al, 2014), at pH 6.5 or neutralized to pH 7.4 (Fig. EV3; Appendix Fig. S3B). Circadian rhythms of BMDMs cultured in cancer cell supernatant at pH 7.4 or pH 6.5 exhibited increased amplitude and lengthened period compared to RPMI control at pH 7.4 or 6.5, respectively, indicating that cancer cell supernatant contains factors that can alter circadian rhythms of BMDMs. Notably, BMDMs cultured in cancer cell supernatant at pH 6.5 had increased amplitude and shortened period compared to BMDMs cultured in cancer cell-conditioned media at pH 7.4, indicating that pH-driven changes in rhythms were maintained in BMDMs cultured in cancer cell supernatant. When the pH of cancer cell supernatant was neutralized to pH 7.4, the increased amplitude was decreased, and the shortened period was lengthened, indicating that neutralizing acidic pH partially reverses the changes in rhythms observed in macrophages cultured in cancer cell supernatant at pH 6.5. These data further support our observations that acidic pH can alter circadian rhythms of macrophages both alone and in combination with various factors in the TME.
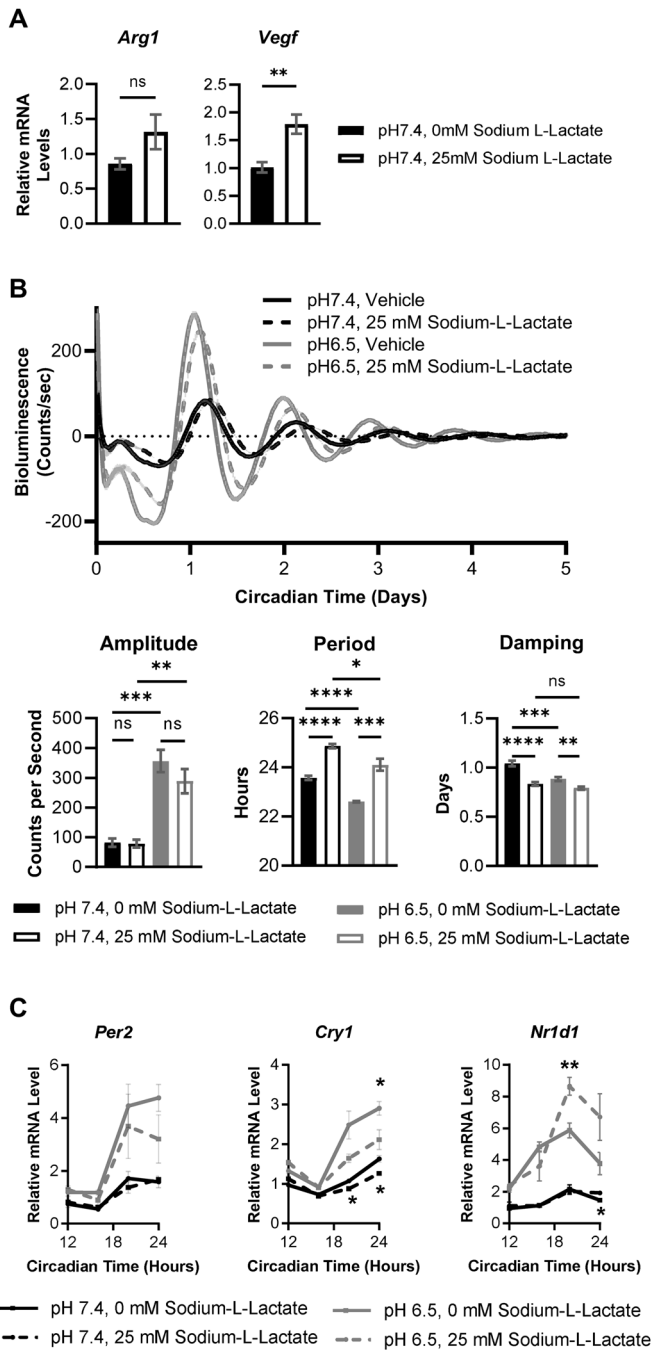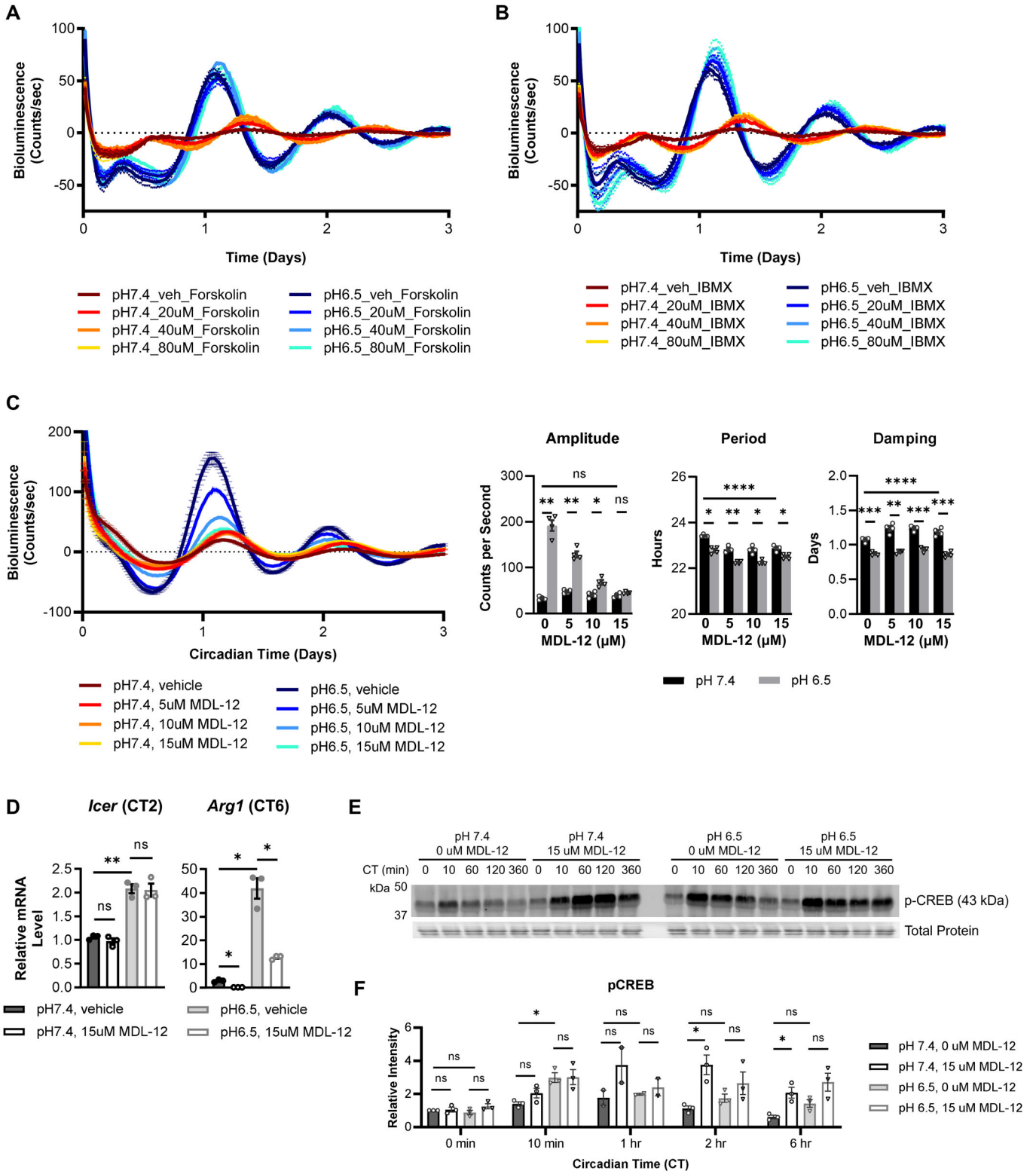
Figure 4. Lactate alters circadian rhythms in macrophages, both alone and in conjunction with acidic pH.

(A–C) Bone marrow-derived macrophages (BMDMs) were obtained from C57BL/6 mice expressing Per2-Luc. The circadian clocks of BMDMs were synchronized by a 24-h period of serum starvation in media with 0% serum, followed by a 2-h period of serum shock in media with 50% serum. BMDMs were then cultured in media with neutral pH 7.4 or acidic pH 6.5, supplemented with 0 mM or 25 mM sodium-L-lactate. (A) RNA was collected at 6 h post-treatment, and expression of pro-resolution phenotype markers *Arg1* or *Vegf* was quantified by qtPCR. $n = 6$ biological replicates. (B) Luciferase activity was monitored in real time by LumiCycle. Data was baseline-subtracted using the running average, $n = 4$ biological replicates. Oscillation parameters were measured by LumiCycle Analysis. Data was pooled from 2 replicated experiments (pH 7.4, 0 mM sodium-L-lactate: $n = 10$. pH 7.4, 25 mM sodium-L-lactate, $n = 10$. pH 6.5, 0 mM sodium-L-lactate: $n = 7$. pH 6.5, 25 mM sodium-L-lactate, $n = 7$, all replicates were biological replicates). (C) RNA was collected at 12, 16, 20, and 24 h post-synchronization, and qt-PCR was performed to assess oscillation of transcripts encoding core clock proteins in macrophages exposed to lactate. Data was pooled from 2 independent replicated experiments. (pH 7.4, 0 mM sodium-L-lactate: $n = 6$. pH 7.4, 25 mM sodium-L-lactate: $n = 6$. pH 6.5, 0 mM sodium-L-lactate: $n = 5$. pH 6.5, 25 mM sodium-L-lactate: $n = 6$, all replicates were biological replicates). Data information: For (A), shown is the mean and SEM, experiment replicated twice. For (B), top panel (LumiCycle traces), shown is the mean and SEM, experiment was replicated twice. For bottom panel (LumiCycle parameter analysis), shown is the mean and SEM. For (C), shown is the mean and SEM. For all panels, statistical significance was determined by unpaired two-tailed t-test with Welch's correction for pH 7.4 0 mM sodium-L-lactate vs 25 mM mM sodium-L-lactate and pH 6.5 0 mM sodium-L-lactate vs 25 mM sodium-L-lactate (other comparisons were not performed on these data). The Holm-Šídák correction for multiple t-tests was applied; $^*p < 0.05$; $^{**}p < 0.005$; $^{***}p < 0.0005$; $^{****}p < 0.0001$; ns: not significant. Exact p values: (A) *Vegf* 0.0045. (B) Amplitude 0.0002 (pH 7.4 0 mM sodium-L-lactate vs pH 6.5 0 mM sodium-L-lactate), 0.0015 (pH 7.4 25 mM sodium-L-lactate vs pH 6.5 25 mM sodium-L-lactate); Period <0.0001 (pH 7.4 0 mM sodium-L-lactate vs pH 6.5 0 mM sodium-L-lactate), <0.0001 (pH 7.4 0 mM sodium-L-lactate vs pH 7.4 25 mM sodium-L-lactate), 0.0209 (pH 7.4 25 mM sodium-L-lactate vs pH 6.5 25 mM sodium-L-lactate), 0.0008 (pH 6.5 0 mM sodium-L-lactate vs pH 6.5 25 mM sodium-L-lactate); Damping 0.0003 (pH 7.4 0 mM sodium-L-lactate vs pH 6.5 0 mM sodium-L-lactate), <0.0001 (pH 7.4 0 mM sodium-L-lactate vs pH 7.4 25 mM sodium-L-lactate), 0.0036 (pH 6.5 0 mM sodium-L-lactate vs pH 6.5 25 mM sodium-L-lactate). (C) *Cry1* 0.04153 (pH 7.4 0 mM sodium-L-lactate vs pH 7.4 25 mM sodium-L-lactate CT 20), 0.00594 (pH 7.4 0 mM sodium-L-lactate vs pH 7.4 25 mM sodium-L-lactate CT 24), 0.028433 (pH 6.5 0 mM sodium-L-lactate vs pH 6.5 25 mM sodium-L-lactate CT 24); *Nr1d1* 0.015989 (pH 7.4 0 mM sodium-L-lactate vs pH 7.4 25 mM sodium-L-lactate CT 20), 0.003984 (pH 6.5 0 mM sodium-L-lactate vs pH 6.5 25 mM sodium-L-lactate CT 20). Some 'ns' have been omitted from (C) for visual clarity.

Induction of cAMP signaling alone is not sufficient to fully drive changes in circadian rhythms associated with acidic pH

Evidence in the literature suggests that acidic pH is primarily sensed by macrophages via certain G protein-coupled receptors (GPCRs), inducing an increase in intracellular cAMP that drives downstream signaling through the cAMP pathway (Bohn et al, 2018). Transcriptional changes downstream of cAMP signaling subsequently promote a pro-resolution phenotype (Bohn et al, 2018; Polumuri et al, 2021; Tavares et al, 2020). Transcription of the *Crem* isoform *Icer* is also induced downstream of cAMP

signaling, and has been used as a "biomarker" for macrophages exposed to acidic conditions in tumors (Bohn et al, 2018). In line with previous reports, we observed induction of *Icer* in macrophages under acidic pH (Fig. EV2B), suggesting that cAMP signaling is being induced under acidic conditions (Bohn et al, 2018). This occurs as early as 2 h, concurrent with changes in rhythms, which are observed by 6 h following exposure to acidic conditions. It has been shown that induction of cAMP signaling alone is sufficient to drive a pro-resolution phenotype in macrophages similar to that observed under acidic conditions (Bohn et al, 2018; Polumuri et al, 2021). In addition, cAMP signaling has been previously observed to modulate circadian rhythms in SCN and rat fibroblasts (O'Neill et al, 2008; Yagita and Okamura, 2000). Thus, we sought to understand if the cAMP signaling pathway may be mediating the pH-induced changes in circadian rhythms in macrophages.

A Bioluminescence (Counts/sec) vs Time (Days)

pH7.4_veh_Forskolin | pH6.5_veh_Forskolin
pH7.4_20uM_Forskolin | pH6.5_20uM_Forskolin
pH7.4_40uM_Forskolin | pH6.5_40uM_Forskolin
pH7.4_80uM_Forskolin | pH6.5_80uM_Forskolin

B Bioluminescence (Counts/sec) vs Time (Days)

pH7.4_veh_IBMX | pH6.5_veh_IBMX
pH7.4_20uM_IBMX | pH6.5_20uM_IBMX
pH7.4_40uM_IBMX | pH6.5_40uM_IBMX
pH7.4_80uM_IBMX | pH6.5_80uM_IBMX

C Bioluminescence (Counts/sec) vs Circadian Time (Days)

Amplitude — Counts per Second vs MDL-12 (µM)
Period — Hours vs MDL-12 (µM)
Damping — Days vs MDL-12 (µM)

pH7.4, vehicle | pH6.5, vehicle
pH7.4, 5uM MDL-12 | pH6.5, 5uM MDL-12
pH7.4, 10uM MDL-12 | pH6.5, 10uM MDL-12
pH7.4, 15uM MDL-12 | pH6.5, 15uM MDL-12

pH 7.4 | pH 6.5

D *Icer* (CT2), *Arg1* (CT6) — Relative mRNA Level

pH7.4, vehicle | pH6.5, vehicle
pH7.4, 15uM MDL-12 | pH6.5, 15uM MDL-12

E Western blot: p-CREB (43 kDa), Total Protein; pH 7.4 0 uM MDL-12, pH 7.4 15 uM MDL-12, pH 6.5 0 uM MDL-12, pH 6.5 15 uM MDL-12; CT (min) 0 10 60 120 360

F pCREB — Relative Intensity vs Circadian Time (CT)

pH 7.4, 0 uM MDL-12
pH 7.4, 15 uM MDL-12
pH 6.5, 0 uM MDL-12
pH 6.5, 15 uM MDL-12

The synchronization protocol we use to study circadian rhythms in BMDMs involves a 24-h period of serum starvation followed by 2 h of serum shock. It has previously been shown that serum shock can induce signaling through the cAMP pathway in rat fibroblasts (Yagita and Okamura, 2000). To determine whether the synchronization protocol impacts cAMP signaling in macrophages, we harvested macrophages before and after serum shock. We then assessed *Icer* expression and phosphorylation of cyclic

Figure 5. pH-induced changes in circadian rhythms are not driven by cAMP signaling alone.

(A, B) Bone marrow-derived macrophages (BMDMs) were obtained from C57BL/6 mice expressing Per2-Luc. BMDMs were cultured in media with neutral pH 7.4 or acidic pH 6.5, and (A) treated with vehicle or 20, 40, or 80 μM Forsokolin, or (B) treated with vehicle or 20, 40, 80 μM IBMX. Luciferase activity was monitored in real time by LumiCycle. Data was baseline-subtracted using the running average, $n = 2$ biological replicates. (C) The circadian clocks of BMDMs were synchronized by a 24-h period of serum starvation in media with 0% serum, followed by a 2-h period of serum shock in media with 50% serum. BMDMs were then cultured in media with neutral pH 7.4 or acidic pH 6.5, and treated with vehicle or 5, 10, or 15 μM MDL-12. Luciferase activity was monitored in real time by LumiCycle. Data was baseline-subtracted using the running average, and oscillation parameters were measured by LumiCycle Analysis, $n = 4$ biological replicates. (D) Expression of the acid sensing gene (Icer) was measured at 2 h post treatment (CT2), and gene associated with a pro-resolution phenotype (Arg1) was measured at 6 h post-treatment (CT6), $n = 3$ biological replicates. (E, F). (E) Phosphorylation of CREB was assessed by immunoblot at the indicated timepoints after synchronization, MDL-12 treatment, and exposure to low pH. (F) Relative pCREB levels from (E) were quantified; band intensity was normalized to total protein, $n = 3$ biological replicates. Data information: For (A, B), shown are individual points and mean. For (C, D, F), mean and SEM are shown. Each experiment was replicated at least two times. For (C, right panels), statistical significance was determined with two-way ANOVA to compare all pH 7.4 vs pH 6.5 data points, and for each individual MDL-12 comparison, unpaired two-tailed t-tests with Welch's correction and the Holm–Šídák correction for multiple t-tests were applied. For (D, F), statistical significance was determined by unpaired two-tailed t-test with Welch's correction (pH 7.4 vehicle vs pH 6.5 15 μM MDL-12 was not tested); *$p < 0.05$; **$p < 0.005$; ***$p < 0.0005$; ****$p < 0.0001$; ns: not significant. Exact P values: Amplitude 0.002346 (pH 7.4 vs pH 6.5 vehicle), 0.002346 (pH 7.4 vs pH 6.5 5 μM MDL-12), 0.01276 (pH 7.4 vs pH 6.5 10 μM MDL-12); Period <0.0001 (pH 7.4 vs pH 6.5 by two-way ANOVA), 0.005197 (pH 7.4 vs pH 6.5 vehicle), 0.003662 (pH 7.4 vs pH 6.5 5 μM MDL-12), 0.005197 (pH 7.4 vs pH 6.5 10 μM MDL-12), 0.005197 (pH 7.4 vs pH 6.5 15 μM MDL-12); Damping <0.0001 (pH 7.4 vs pH 6.5 by two-way ANOVA), 0.000307 (pH 7.4 vs pH 6.5 vehicle), 0.00119 (pH 7.4 vs pH 6.5 5 μM MDL-12), 0.000105 (pH 7.4 vs pH 6.5 10 μM MDL-12), 0.000307 (pH 7.4 vs pH 6.5 15 μM MDL-12). (D) Icer 0.0053 (pH 7.4 vehicle vs pH 6.5 vehicle); Arg1 0.0148 (pH 7.4 vehicle vs pH 7.4 15 μM MDL-12), 0.0117 (pH 7.4 vehicle vs pH 6.5 vehicle), 0.0202 (pH 6.5 vehicle vs pH 6.5 15 μM MDL-12). (F) 10 min 0.01823 (pH 7.4 vs pH 6.5 0 μM MDL-12); 2 hr 0.03913 (pH 7.4 0 μM MDL-12 vs pH 7.4 15 μM MDL-12); 6 hr 0.036106 (pH 7.4 0 μM MDL-12 vs pH 7.4 15 μM MDL-12).

AMP-response element binding protein (CREB), which occur downstream of cAMP and have been used as readouts to assess induction of cAMP signaling in macrophages (Bohn et al, 2018; Misra and Pizzo, 2005; Polumuri et al, 2021). Serum shock of macrophages following serum starvation led to rapid phosphorylation of CREB and Icer expression that quickly returned to baseline (Fig. EV1D,E). This indicates that serum starvation followed by serum shock in the synchronization protocol we use to study circadian rhythms in BMDMs induces transient signaling through the cAMP signaling pathway.

As acidic pH induces signaling through the cAMP pathway, we sought to determine whether acidic pH independently contributed to the pH-driven changes in circadian rhythms we observe in BMDMs. To test this, we omitted the synchronization step and observed BMDM rhythms by LumiCycle when cultured in neutral pH 7.4 or acidic pH 6.8 or pH 6.5 (Fig. EV4). Circadian rhythms of BMDMs cultured at pH 6.5 exhibited similar changes as previously observed, with enhanced amplitude and shortened period relative to BMDMs at pH 7.4. This indicates pH-driven changes observed in circadian rhythms of BMDMs occur in the absence of prior serum starvation and serum shock.

To determine if elevation in intracellular cAMP alone was sufficient to drive changes in rhythms observed in macrophages under acidic conditions, we treated macrophages with forskolin, an adenylyl cyclase activator that stimulates production of cAMP, or 3-isobutyl-1-methylxanthine (IBMX), which drives accumulation of cAMP through inhibition of phosphodiesterases (PDEs). We used a range of doses similar to those previously shown to induce cAMP signaling in macrophages in the literature (Bohn et al, 2018; Misra and Pizzo, 2005; Yagita and Okamura, 2000). Treatment with either forskolin or IBMX increased amplitude of rhythms in macrophages, but not to the same magnitude as acidic pH, and did not result in a changed period (Fig. 5A,B). Moreover, amplitude of rhythms was not altered in forskolin- or IBMX-treated macrophages at pH 6.5, indicating that neither forskolin nor IBMX had any additional effect on rhythms under acidic conditions. These data indicate that in macrophages, cAMP signaling alone induces enhanced amplitude of rhythms similar to low pH, but the

magnitude of this change is far less; additionally, period, which is altered under acidic conditions, remains unchanged. This suggests that cAMP signaling may contribute to but is not sufficient to fully recapitulate the changes in rhythms observed under acidic conditions.

Adenylyl cyclase inhibitor MDL-12330A suppresses pH-mediated changes in amplitude of circadian rhythms and pro-resolution phenotype without suppressing cAMP signaling

To further test whether pH-induced changes in rhythms are mediated by cAMP signaling, we treated BMDMs with MDL-12330A (henceforth referred to as MDL-12), an adenylyl cyclase inhibitor which has previously been shown to suppress cAMP signaling in macrophages under acidic conditions (Bohn et al, 2018). When BMDMs cultured at pH 6.5 were treated with MDL-12, the elevated amplitude of rhythms observed at pH 6.5 was suppressed (Fig. 5C; Appendix Fig. S3C). Notably, this occurred in a dose-dependent manner, suggesting that this is a drug-dependent effect. Importantly, rhythms of MDL-12-treated macrophages at pH 7.4 had similar amplitude to vehicle-treated macrophages at pH 7.4. This suggests that the inhibitory effect of MDL-12 on pH-induced enhancement of amplitude in macrophage rhythms was specific to acidic conditions. However, MDL-12 treatment of macrophages at pH 7.4 resulted in shortened period and decreased damping rate compared to vehicle-treated macrophages. Together, MDL-12-mediated suppression of pH-driven changes in amplitude, but not period or damping, suggests that the pH-driven changes in these different parameters of rhythms may occur through different pathways. Interestingly, although the adenylyl cyclase inhibition by MDL-12 is reported to be irreversible, we found that pre-treatment up to 2 h was not sufficient to suppress pH-induced changes in amplitude (Appendix Fig. S4). Only when macrophages continued to be cultured with MDL-12 while exposed to acidic conditions was amplitude suppressed. Meanwhile, co-treating cells with acidic pH and MDL12 without any pre-treatment was sufficient to suppress elevation of amplitude under acidic conditions (Fig. 5C).

A *Arg1*

B Reference Correlation

C Bone Marrow-Derived Macrophages · Peritoneal Macrophages WT · Peritoneal Macrophages BMAL1 KO · Tumor-Associated Macrophages

Crem

D

E Peritoneal Macrophages WT · Peritoneal Macrophages BMAL1 KO · Tumor-Associated Macrophages
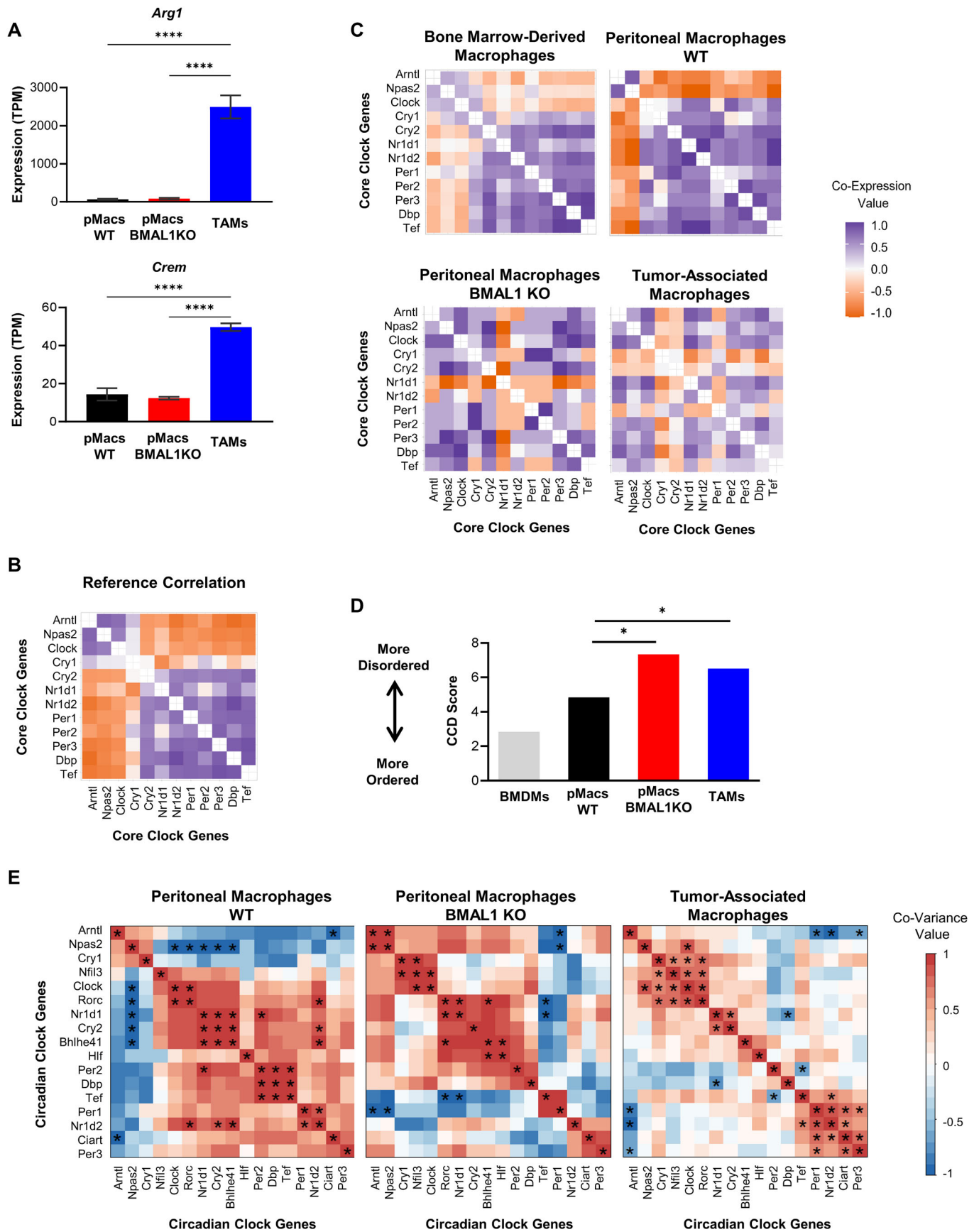
Figure 6. Clock correlation distance (CCD) and weighted gene co-expression network analysis (WGCNA) provide evidence of circadian disorder in murine tumor-associated macrophages.

(A) RNAseq datasets (see **Methods**) of WT peritoneal macrophages (pMac), BMAL1 KO peritoneal macrophages, and tumor-associated macrophages (TAMs) were analyzed for expression of *Arg1* and *Crem* (WT pMac: $n = 5$. BMAL1KO pMac: $n = 4$. TAMs: $n = 10$, all replicates are biological replicates). (B) A pan-tissue murine reference control was used for clock correlation distance (CCD). (C, D). (C) Clock correlation distance (CCD) analysis was performed and (D) statistical analysis to compare CCD scores was performed by calculating delta CCD. For BMDMs, $n = 72$ biological replicates, for all other conditions, see (A). (E) Weighted gene co-expression network analysis (WGCNA) was performed on the indicated circadian clock genes using data from (A–D). Data information: For (A), mean and SEM are shown. Statistical significance was determined with Ordinary one-way ANOVA with Tukey's multiple comparisons test, ****$p < 0.0001$ for each indicated comparison. For (D), *$p < 0.05$ by delta CCD analysis compared to control group only (pMacs WT). For (E), *$p < 0.05$ by WGCNA for significant covariance by Pearson correlation, and blank squares are not significant. Exact p values: (D) 0.00802 (pMacs WT vs pMacs BMAL1KO), 0.007826 (pMacs WT vs TAMs).

Evidence suggests that acidic pH signals through the cAMP pathway to promote a pro-resolution phenotype in macrophages, with induction of *Icer* occurring directly downstream of cAMP signaling (Bohn et al, 2018). Despite preventing changes in amplitude under acidic pH, MDL12 treatment at the dose and treatment schedule used does not suppress induction of *Icer* in macrophages under acidic conditions (Fig. 5D). However, induction of *Arg1* expression in macrophages under acidic conditions was suppressed by MDL-12. This suggests that at the dose and treatment strategy used, MDL-12 partially suppresses the response of macrophages to acidic pH by suppressing the pH-driven polarization toward a pro-resolution phenotype and changes in amplitude.

To further investigate how MDL-12 was influencing cAMP signaling at the dose and treatment strategy used, we evaluated phosphorylation of cyclic AMP-response element binding protein (CREB). Phosphorylation of CREB occurs downstream of cAMP and has commonly been used as a readout to assess induction of cAMP production in macrophages (Misra and Pizzo, 2005; Polumuri et al, 2021). In line with evidence in the literature that exposure to acidic pH drives an increase in intracellular cAMP in macrophages (Bohn et al, 2018), we observed that downstream phosphorylation of CREB was elevated in macrophages exposed to acidic pH compared to those in non-acidic conditions (Fig. 5E,F). Unexpectedly, pCREB levels remained elevated in BMDMs at pH 6.5 despite treatment with MDL-12, indicating that pH-driven phosphorylation of CREB was not suppressed by MDL12 treatment. In fact, pCREB was elevated in MDL-12-treated BMDMS at pH 7.4, suggesting that MDL-12 treatment alone induced phosphorylation of CREB. This is particularly surprising considering that amplitude was not altered in MDL-12-treated macrophages at neutral pH 7.4 despite elevated pCREB. This suggests that some elements of the cAMP signaling pathway, such as pCREB, may be divorced from the pH-induced changes in rhythms. Collectively, our data indicate that while the cAMP signaling pathway is induced under acidic conditions, pH-induced changes in rhythms may not be attributable to cAMP signaling alone, as MDL-12 treatment suppressed pH-induced changes in amplitude of rhythms, but not period or damping, without suppressing signaling through the cAMP pathway.

There is evidence of circadian disorder in the tumor-associated macrophage population

As we have observed that acidic pH at levels commonly observed in the TME can alter circadian rhythms in macrophages in vitro and ex vivo, we next sought to investigate whether circadian rhythms can be altered in the TME in vivo. Using publicly available data, we analyzed gene expression of tumor-associated macrophages (TAMs) isolated from LLC (Lewis Lung carcinoma) tumors in mice (Geeraerts et al, 2021a, b). As a positive control for circadian clock disruption, we used data from BMAL1 KO peritoneal macrophages (Kitchen et al, 2019; Kitchen et al, 2020). BMAL1 KO macrophages have a genetic disruption of the circadian clock due to the loss of Bmal1, the central clock gene. As a result, circadian rhythms of BMAL1 KO macrophages are disrupted, lacking rhythmicity and downstream circadian regulation of macrophage function (see Fig. 10A,B) (Curtis et al, 2015; Gibbs et al, 2012). In line with previous observations, TAMs had elevated expression of *Arg1* relative to WT and BMAL1 KO peritoneal macrophages (Fig. 6A). Expression of *Crem*, which encodes *Icer*, was also elevated in TAMs, indicating that these TAMs were exposed to acidic conditions within the TME (Fig. 6A) (Bohn et al, 2018).

To understand the status of the circadian clock in TAMs, we performed clock correlation distance (CCD) analysis. This analysis has previously been used to assess functionality of the circadian clock in whole tumor and in normal tissue (Shilts et al, 2018). As the circadian clock is comprised of a series of transcription/translation feedback loops, gene expression is highly organized in a functional, intact clock, with core clock genes existing in predictable and ordered levels relative to each other irrespective of the time of day. In a synchronized population of cells, this ordered relationship is maintained at the population level, which can be visualized in a heatmap. CCD is designed to compare circadian clock gene co-expression patterns between different tissues and cell types. To accomplish this, CCD was built using datasets from multiple different healthy tissues from mouse and human to be a universal tool to compare circadian rhythms. Each sample is compared to a reference control built from these multiple tissues (Fig. 6B) (Shilts et al, 2018). To validate the use of this analysis for assessing circadian disorder in macrophages, we performed CCD analysis using publicly available RNA-sequencing data from bone marrow-derived macrophages (Collins et al, 2020; Collins et al, 2021) and wild-type peritoneal macrophages (Kitchen et al, 2019, 2020) as healthy controls for functional rhythms in synchronized cell populations, and BMAL1 KO peritoneal macrophages as a positive control for circadian disorder (Kitchen et al, 2019, 2020). We found that gene co-expression of clock genes was ordered in wild-type macrophages with functional clocks and intact circadian rhythms (Fig. 6C). In contrast, clock gene co-expression was disordered in BMAL1 KO macrophages with a genetic disruption of the circadian clock, leading to disruption of circadian rhythms (Fig. 6C,D). This indicates that CCD analysis can be used to measure circadian disorder in a macrophage population. To assess the status of the circadian clock in tumor-associated macrophages, we next performed CCD analysis using RNA-sequencing data of TAMs derived from LLC tumors (Geeraerts et al, 2021a, b). Clock correlation distance analysis revealed
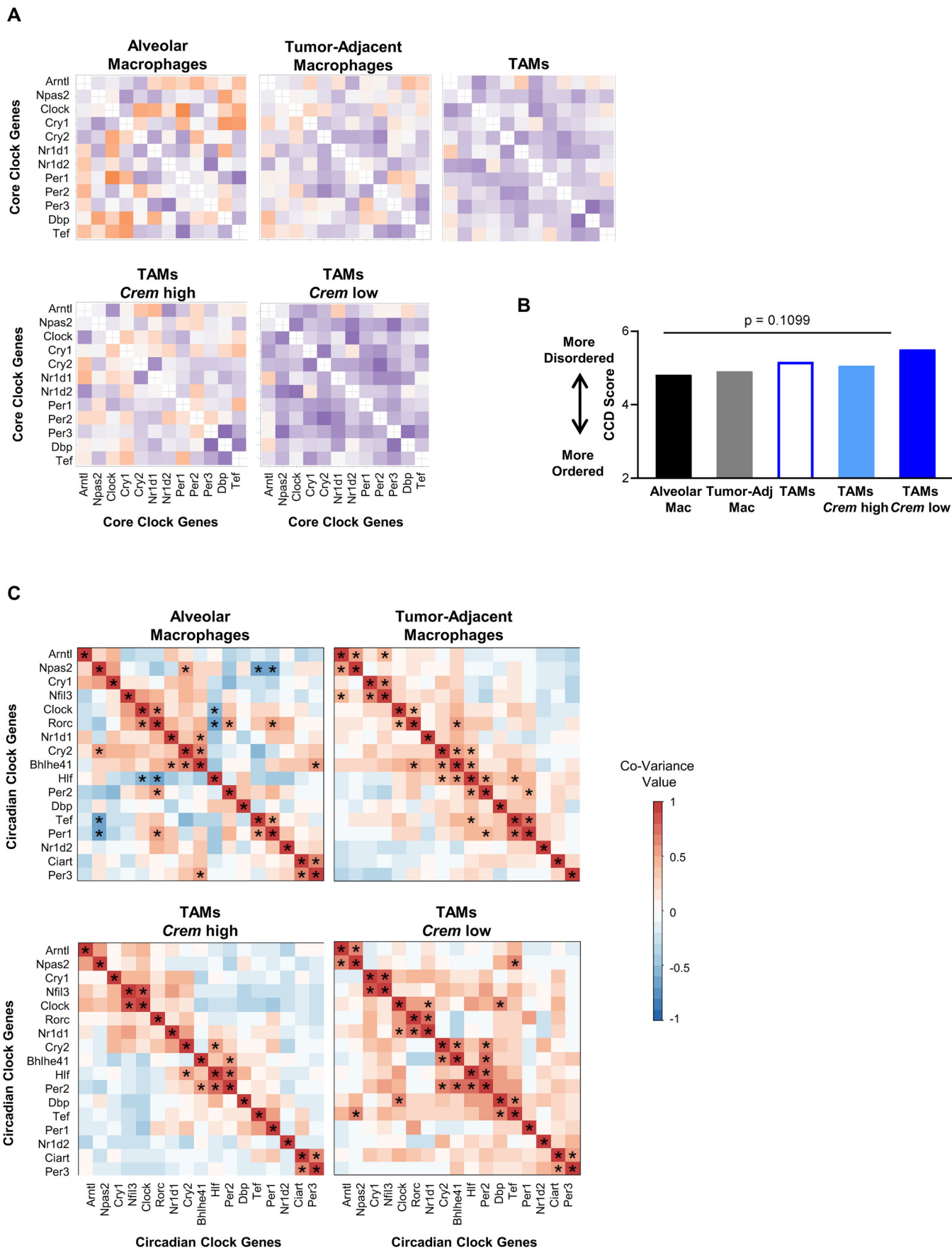
Figure 7. Clock correlation distance (CCD) and weighted gene co-expression network analysis (WGCNA) provide evidence of circadian disorder in human tumor-associated macrophages.

(A) Clock correlation distance (CCD) analysis was performed using RNAseq datasets of macrophages from tumor (TAMs, $n = 40$ patients), tumor-adjacent tissue from NSCLC patients ($n = 34$ patients), and alveolar macrophages from healthy donors ($n = 24$ donors) (see Methods for information on these samples). TAM samples were subset by median *Crem* expression into *Crem* high TAM samples (TAMs *Crem* high, $n = 20$ patients) and *Crem* low TAM samples (TAMs *Crem* low, $n = 20$ patients). (B) Statistical analysis to compare CCD scores was performed by calculating delta CCD, with $p < 0.05$ being deemed significantly different from the control group. (C) Weighted gene co-expression network analysis (WGCNA) was performed on the indicated circadian clock genes using data from (A, B). Data information: For (B), p value shown is by delta CCD analysis compared to control group. For (C), *$p < 0.01$ by WGCNA for significant covariance by Pearson correlation, and blank squares are not significant.

that, similar to the BMAL1 KO peritoneal macrophages, the co-expression relationship between the core circadian clock genes in TAMs was significantly more disordered than that of WT peritoneal macrophages (Fig. 6C,D). Weighted gene co-expression network analysis (WGCNA) has been used as an alternate approach to measure the covariance between clock genes and thus assess bi-directional correlations among the core clock gene network in healthy tissue and tumor samples (Chun et al, 2022). In line with the circadian disorder observed by CCD, while many bi-directional correlations among the core clock gene network were significant and apparent in wild type peritoneal macrophages, these relationships were altered or abolished within BMAL1 KO peritoneal macrophages and TAM samples, and in some cases replaced by new relationships (Fig. 6E). This indicates that there is population-level disorder in the circadian rhythms of tumor-associated macrophages in murine lung cancer.

We next assessed the status of the circadian clock in human TAMs from NSCLC patients. We performed CCD with publicly available RNA-seq data of tumor-adjacent macrophages and tumor-associated macrophages from NSCLC patients, using alveolar macrophages from healthy donors as a control (Garrido-Martin et al, 2020a, b; Shaykhiev et al, 2009a, b). To assess the contribution of the acidic TME to circadian disorder, we subset TAM NSCLC patient samples into groups (*Crem* high TAMs and *Crem* low TAMs) based on median *Crem* expression. Notably, in macrophages from human NSCLC there was a trend toward disorder in *Crem* low but not *Crem* high TAM samples (Fig. 7A,B). In addition, the covariance among core clock genes observed in alveolar macrophages from healthy donors was absent within *Crem* low and *Crem* high TAM samples (Fig. 7C). In all, these data indicate that there is population-level disorder in the circadian rhythms of tumor-associated macrophages in humans and mice, suggesting that circadian rhythms are indeed altered in macrophages within the TME.

Heterogeneity of circadian rhythms within a population can underlie circadian disorder as measured by CCD

Circadian disorder assessed by CCD has previously been used to infer disruption of circadian rhythms (Pariollaud et al, 2022). Indeed, we observed that genetic disruption of circadian rhythms by BMAL1 KO resulted in a disordered clock, as observed in peritoneal macrophages (Fig. 6B). However, since CCD is a population-level analysis, heterogeneity of rhythms, as observed in a desynchronous cell population, rather than disruption of rhythms, may also underlie the circadian disorder observed by CCD. Heterogeneity in macrophage phenotype, exposure to acidic pH, and lactate are all factors present in the TME and relevant to tumor-associated macrophages. We observed that each of these factors can alter circadian rhythms in macrophages, both alone and

in combination with each other. Furthermore, we observed a trend toward circadian disorder in *Crem* low TAM samples but not *Crem* high TAM samples. Thus, we sought to understand if heterogeneity in macrophage rhythms could be contributing to the disorder in clock gene co-expression and poor CCD score indicative of population-level disorder in TAM rhythms.

To address this, we examined if differences in rhythms of macrophages within a population might contribute to population-level disorder as measured by CCD. To this end, we used publicly available data of peritoneal macrophages taken at different times of day in 4-h intervals across 2 days (Keller et al, 2009; Keller et al, 2010). We then constructed four different sample groups in which samples were pooled according to time of day of harvest. As a control for a synchronized cell population with homogenous rhythms, samples taken at the same time of day were pooled. We then modeled a progressively desynchronized population with increased differences in phase of rhythms by pooling samples that were taken 4 h apart, 8 h apart, or 12 h apart (Fig. 8A). CCD was performed on these four populations (Fig. 8B). CCD score worsened as populations became increasingly desynchronized, with the 12 h desynchronized population having a significantly worse CCD score than synchronized, homogenous macrophage population (Fig. 8C). This indicates that as circadian rhythms of individual macrophages within a population become more different from each other, circadian disorder increases at the population-level. This is further supported by WGCNA, which revealed that the significant covariance of circadian clock genes in the synchronized population was progressively altered and lost as the population is increasing desynchronized to 12 h (Fig. EV5). The results of these analyses suggest that heterogeneity in rhythms, as observed with desynchrony, may underlie population-level disorder of the circadian clock as measured by CCD.

Tumor-associated macrophages exhibit heterogeneity in circadian clock gene expression

Our findings suggested that heterogeneity of the circadian clock may lead to disorder in bulk macrophage populations, but did not reveal if specific gene expression changes exist in tumor-associated macrophages at the single-cell level. To determine whether heterogeneity exists within the expression of circadian clock genes of the tumor-associated macrophage population, we analyzed publicly available single-cell RNA-sequencing data of macrophages isolated from B16-F10 tumors (Wang et al, 2024a, b). To capture the heterogeneity of macrophage subsets within the TAM population, we performed unbiased clustering (Fig. 9A). We then performed differential gene expression to determine if circadian clock genes were differentially
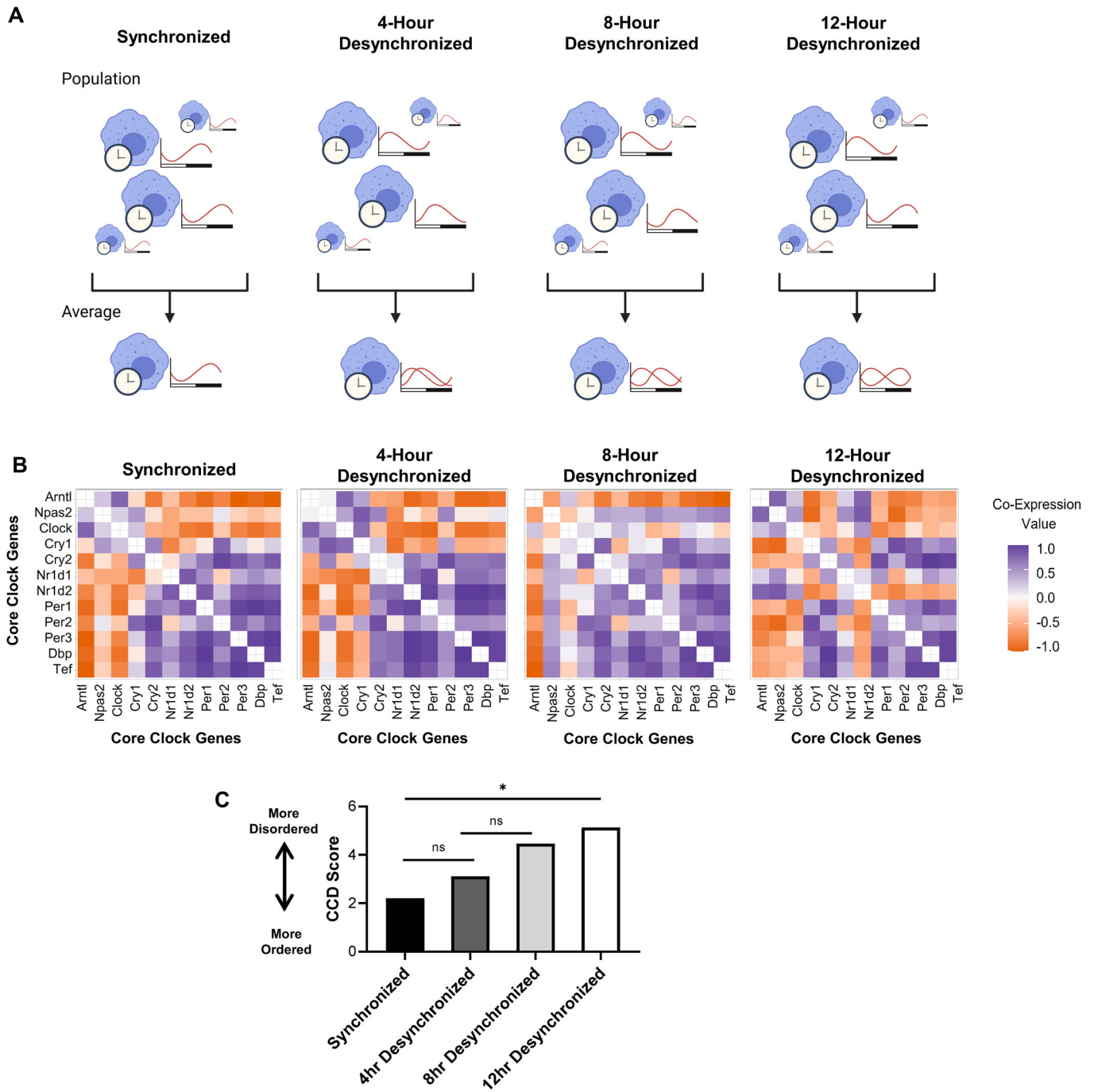
Figure 8. Heterogeneity in circadian rhythms of cells within a population can lead to circadian disorder observed by CCD.

(A–C) Increasingly desynchronized populations were modeled using an RNAseq data set of WT peritoneal macrophages (n = 12 biological replicates) taken at 4-h intervals across two days (see Methods). (A) A schematic of the populations used in experimental design. (B, C) (B) Clock correlation distance (CCD) analysis was performed and (C) statistical analysis to compare CCD scores was performed by calculating delta CCD. Data information: *p < 0.05 by delta CCD analysis compared to control group. Exact p values: (C) 0.016442 (Synchronized vs 12 h Desynchronized).

expressed within the TAM subpopulations. The circadian clock genes *Bhlhe40* (DEC1), *Bhlhe41* (DEC2), *Nfil3* (E4BP4), *Rora* (RORα), *Dbp* (DBP), and *Nr1d2* (REV-ERBβ) were significantly (adj.p < 0.005) differentially expressed between TAM clusters (Fig. 9B; Appendix

Table S1A). This indicates that there is heterogeneity in expression of circadian clock genes within the TAM population.

We next sought to determine whether differences in circadian clock gene expression between TAM subpopulations were associated with
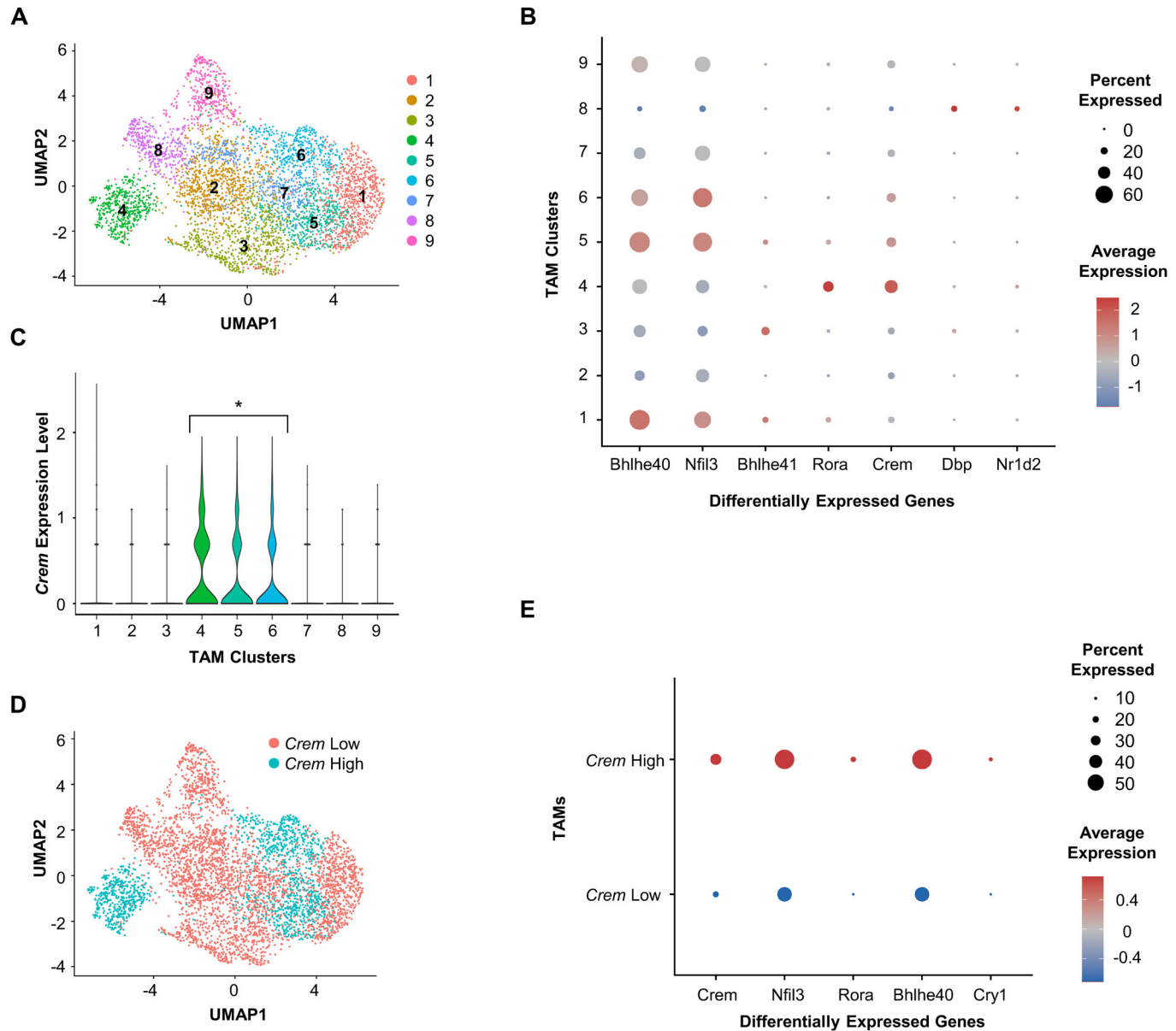
Figure 9. There is heterogeneity in expression of circadian clock genes within the tumor-associated macrophage population.

We analyzed a single-cell RNAseq dataset of tumor-associated macrophages (see Methods for information on these samples). (A) Unbiased clustering was performed to identify TAM subpopulations. (B) Differential gene expression analysis was performed on these TAM clusters, and expression of significantly different circadian genes was plotted along with *Crem*. (C) Crem expression of macrophages in TAM clusters was measured. (D) TAMs were subset by *Crem* expression into *Crem* high TAMs and *Crem* low TAMs, and these groups were overlaid on the UMAP plot shown in (A). (E) Differential gene expression analysis was performed on *Crem* high vs *Crem* low, and expression of significantly different circadian genes was plotted. Data information: All differentially expressed genes or groups of clusters in (B), (C), and (E) are adj.p < 0.005 by limma implementation of the Wilcoxon Rank-Sum test. Exact *P* value: (C) 2.71 E-27 (*Crem*-low clusters vs *Crem*-high clusters). Exact *P* values for (B, E) are available in Appendix Fig. S4.

exposure to acidic pH in the TME. To this end, we first assessed *Crem* expression in the TAM subpopulations that were identified by unbiased clustering. *Crem* expression was significantly higher in TAM clusters 4, 5, and 6 compared to TAM clusters 1–3 and 7–9 (Fig. 9C). Clusters were subset based on *Crem* expression into *Crem* high (clusters 4–6) and *Crem* low (clusters 1–3, 7–9) (Fig. 9D), and differential gene expression analysis was performed. The circadian clock genes *Nfil3, Rora, Bhlhe40*, and *Cry1* (CRY1) were significantly (adj.p < 0.005) differentially

expressed between *Crem* high and *Crem* low TAMs (Fig. 9E; Appendix Table S1B). This suggests that acidity within the TME is associated with heterogeneity in expression of circadian clock genes within the TAM population. Interestingly, expression of circadian clock genes varied between clusters designated as *Crem* high or *Crem* low (Fig. 9B); for instance, *Nfil3* was more highly expressed in cluster 1 than cluster 3, both of which had low *Crem* expression. This indicates that there is diversity in circadian clock gene expression within the *Crem* high and

Figure 10. A functional circadian clock in macrophages can influence tumor growth in a murine model of PDAC.

(A) Levels of Bmal1 in bone marrow-derived macrophages (BMDMs) from WT or BMAL1 KO mice were assessed by immunoblot. (B) To confirm functional disruption of the circadian clock, peritoneal macrophages or BMDMs were obtained from WT or BMAL1 KO mice expressing PER2-Luc and cultured in vitro with D-luciferin. Luciferase activity was monitored in real time by LumiCycle, $n = 2$ biological replicates. (C, D) (C) Illustration and (D) results of in vivo tumor growth experiment. Bone marrow-derived macrophages (BMDMs) obtained from WT or BMAL1 KO mice were subcutaneously co-injected with KCKO cells into the flank of WT mice. Tumor growth was measured by caliper, $n = 20$ individual mice, 10 male and 10 female. Data information: For (A, B), experiment was replicated twice, and for (B), shown are individual points and mean. For (D), shown is the mean and SEM. Statistical significance determined at each time point by multiple Mann–Whitney tests with two-stage step-up (Benjamini, Krieger, and Yekutieli) correction for multiple testing; *$p < 0.05$; **$p < 0.005$; ***$p < 0.0005$ with $q < 0.05$ for all tests; ns: not significant. Experiment was replicated twice. Exact p values: (D) 0.00321 (16 days), 0.000696 (24 days), 0.016898 (26 days).

murine model of PDAC (Besmer et al, 2011; Kidiyoor et al, 2014). To this end, we used a genetic disruption of the circadian clock in macrophages by deletion of BMAL1 (Fig. 10A,B). Myeloid-specific genetic mouse models are not macrophage-specific, so co-injection experiments are commonly used to determine macrophage-specific roles (Alexander et al, 2020; Colegio et al, 2014; Lee et al, 2018; Mills et al, 2019). Thus, we co-injected BMDMs from WT or BMAL1 KO mice along with KCKO cells into WT mice, and tumor growth was measured (Fig. 10C). We saw a significant increase in the growth of tumors co-injected with BMAL1 KO macrophages compared to those co-injected with WT macrophages (Fig. 10D). These results suggest intact circadian rhythms of macrophages can restrain tumor growth, in agreement with similar published findings in a murine model of melanoma (Alexander et al, 2020).

Discussion

Macrophages experience altered environmental conditions within the tumor microenvironment, but how these may affect macrophage circadian rhythms remains unclear. Here we assessed whether circadian rhythms are altered in macrophages within the TME. To this end, we investigated whether conditions commonly associated with the tumor microenvironment could influence circadian rhythms in macrophages. As TAMs are phenotypically heterogenous, we first assessed circadian rhythms in macrophages polarized toward different phenotypes. We found that polarization state affected circadian rhythmicity, with pro-inflammatory macrophages exhibiting far weaker rhythms that pro-resolution macrophages (Fig. 1). We then modeled acidic conditions in the TME by exposing macrophages to pH and lactate levels similar to those found in the TME, and found that low pH in particular dramatically altered the rhythms of macrophages (Figs. 2–4, EV3 and EV4). Changes in cAMP signaling may contribute to these changes in rhythmicity, but low pH induced alterations far beyond what is observed by enhancing cAMP signaling pharmacologically (Fig. 5A,B). While the adenylyl-cyclase inhibitor MDL-12 largely rescued the changes in amplitude observed in low pH, our data suggest that a pathway other than canonical cAMP signaling may be involved in this effect (Fig. 5C–F). Finally, we assessed the status of the

Crem low groups, suggesting that acidic pH is not the only factor in the TME that can alter the circadian clock. Collectively, these data suggest that there is heterogeneity in the circadian clock of macrophages within the TAM population that is driven in part by acidic pH.

Circadian rhythms of macrophages can influence tumor growth in a murine model of pancreatic cancer

We next sought to determine how circadian rhythms in tumor-associated macrophages may influence tumor growth in KCKO, a

circadian clock in tumor-associated macrophages, the potential contribution of heterogeneity in circadian rhythms to population-level rhythms, and assessed whether the circadian regulation of macrophages impacts tumor growth. Our results indicated that macrophage rhythms are disordered within tumors (Figs. 6 and 7), and that heterogeneity in rhythms within the tumor-associated macrophage population may underlie this observed circadian disorder (Figs. 8 and EV5), which was supported by our observations of heterogeneity in circadian clock gene expression within the TAM population from scRNA-sequencing data (Fig. 9). We further demonstrated that the intact macrophage circadian clock can suppress tumor growth (Fig. 10). Overall, our results for the first time demonstrate that exposure of macrophages to conditions associated with the tumor microenvironment can influence circadian rhythms, a key aspect of macrophage biology (Synopsis).

A critical question in understanding the role of circadian rhythms in macrophage biology is how different polarization states of macrophages affect their internal circadian rhythms. This is especially important considering that tumor-associated macrophages are a highly heterogeneous population. Our data indicate that compared to unstimulated macrophages, rhythms are enhanced in pro-resolution macrophages, characterized by increased amplitude and improved ability to maintain synchrony; in contrast, rhythms are suppressed in pro-inflammatory macrophages, characterized by decreased amplitude and impaired ability to maintain synchrony (Fig. 1). These agree with previously published work showing that polarizing stimuli alone and in combination with each other can alter rhythms differently in macrophages (Chen et al, 2020; Lellupitiyage Don et al, 2022). In a tumor, macrophages exist along a continuum of polarization states and phenotypes (Chevrier et al, 2017; Cuccarese et al, 2017; Huang et al, 2019; Laviron et al, 2022; Mantovani et al, 2022). Thus, while our characterizations of rhythms in in vitro-polarized macrophages provide a foundation for understanding how phenotype affects circadian rhythms of macrophages, further experiments will be needed to assess macrophages across the full spectrum of phenotypes. Indeed, alteration of rhythms may be just as highly variable and context-dependent as phenotype itself.

In addition to polarizing stimuli, tumor-associated macrophages are exposed to a variety of conditions within the tumor microenvironment that may alter their circadian rhythms. We observed that exposure to acidic pH altered rhythms in macrophages, increasing amplitude of pro-resolution macrophages but suppressing amplitude of pro-inflammatory macrophages (Fig. 2). This indicates that pH affects rhythms differently depending on phenotype, hinting at additional layers of complexity in how the environment could contribute to changes in circadian rhythms. Even further changes in rhythms were observed when macrophages were exposed to stimuli such as lactate or cancer cell supernatant in conjunction with acidic pH (Figs. 4 and EV3). These observations suggest that the combination of stimuli present in the microenvironment such as lactate and low pH, as well as various polarizing stimuli, can each contribute to modulate rhythms, resulting in highly context-dependent changes in circadian rhythms of macrophages based on the microenvironment. As macrophages are highly plastic and exquisitely capable of sensing and responding to their environment, one could reason that changes in circadian rhythms, and downstream circadian regulation, are a mechanism by which macrophages can adopt different programs to respond to their environment.

Elucidating the role of circadian rhythms in regulation of macrophage biology necessitates a better understanding of the crosstalk between phenotype, altered environmental conditions, and circadian rhythms. The differences in response to acidic pH between pro-inflammatory and pro-resolution macrophages (Figs. 1 and 2) may be due to signaling pathways downstream of polarization that directly influence circadian clock gene expression. One previously published finding that may offer mechanistic insight into how phenotype can influence circadian rhythms is the suppression of BMAL1 by LPS-inducible miR-155 (Curtis et al, 2015). It has also been observed that RORα-mediated activation of BMAL1 transcription is enhanced by PPARγ co-activation (Liu et al, 2007). In macrophages, PPARγ expression is induced upon stimulation with IL-4 and plays a key role in alternative activation of macrophages, promoting a pro-resolution macrophage phenotype, and supporting resolution of inflammation (Daniel et al, 2018; Gautier et al, 2012; Odegaard et al, 2007). In addition, lactate polarizes macrophages toward a pro-resolution phenotype similar to acidic pH (Colegio et al, 2014; Jiang et al, 2021b), and we found that exposure to lactate had different effects on circadian rhythms —and in some cases, circadian clock gene expression—than exposure to acidic pH (Fig. 4). Sensing of lactate occurs through different pathways than acid-sensing, which may contribute to the different ways in which these two stimuli modulate circadian rhythms of macrophages (Certo et al, 2022). Such observations prompt the question of whether there are yet-unidentified factors induced downstream of various polarizing stimuli that can modulate expression of circadian genes at the transcriptional and protein levels. Further work is required to understand the interplay between macrophage phenotype, altered environmental conditions, and circadian rhythms.

It was previously observed that acidic pH can disrupt circadian rhythms in cell lines (Walton et al, 2018). However, while acidic pH altered rhythms in macrophages, it did not ablate them. This suggests that the influence of acidic pH on circadian rhythms can vary between cell types. pH-induced circadian disruption was found to be driven by inhibition of mTORC1 activity in cell lines, and there was evidence to suggest that mTORC1 activity was sensitive to pH in T cells (Walton et al, 2019). Thus, the role of mTORC1 activity in mediating pH-driven changes in circadian rhythms of macrophages will be a topic of future investigation.

The mechanism through which acidic pH can modulate the circadian clock in macrophages remains unclear. Evidence in the literature suggests that acidic pH promotes a pro-resolution phenotype in macrophages by driving signaling through the cAMP pathway (Bohn et al, 2018). It has previously been shown that cAMP signaling can modulate the circadian clock (O'Neill et al, 2008). However, our data indicated that cAMP signaling was not fully sufficient to confer pH-mediated changes in circadian rhythms of macrophages (Fig. 5A,B). Treatment with MDL-12, commonly known as an inhibitor of adenylyl cyclase (Bohn et al, 2018; Guellaen et al, 1977), resulted in suppression of pH-induced changes in amplitude of circadian rhythms but did not inhibit signaling through the cAMP signaling pathway (Fig. 5C,D). While MDL-12 is commonly used as an adenylyl cyclase inhibitor, it has also been documented to have inhibitory activity toward phosphodiesterases (PDEs) and the import of calcium into the cytosol through various mechanisms (Hunt and Evans, 1980; van Rossum et al, 2000). This is of particular interest, as calcium signaling has

also been shown to be capable of modulating the circadian clock (O'Neill and Reddy, 2012). Furthermore, while acid-sensing through GPCRs has been the most well-characterized pathway in macrophages, there remain additional ways in which acidic pH can be sensed by macrophages such as acid-sensing ion channels (Ni et al, 2018; Selezneva et al, 2022). Further work is required to understand the signaling pathways through which pH can influence macrophage phenotype and circadian rhythms.

We observed that acidic pH appears to enhance circadian rhythms of unstimulated and pro-resolution macrophages, and we and others have shown evidence that macrophages are exposed to an acidic environment within the TME (Bohn et al, 2018; El-Kenawi et al, 2019). Interestingly, analysis of TAMs by clock correlation distance (CCD) presents evidence that rhythms are disordered in bulk TAMs compared to other macrophage populations (Fig. 6). CCD is one of the most practical tools currently available to assess circadian rhythms due to its ability to assess rhythms independent of time of day and without the need for a circadian time series, which is often not available in publicly available data from mice and humans (Shilts et al, 2018). However, CCD is limited in that it is a measure of population-level circadian rhythms. Our data indicate that heterogeneity of circadian rhythms within a given population can underlie circadian disorder observed by CCD (Figs. 8 and EV5). Indeed, we observed differences in the circadian clock of *Crem* low human TAM samples compared to *Crem* high human TAM samples, suggesting that acidic pH influences circadian disorder in TAMs (Fig. 7). Interestingly, *Crem* low TAM samples exhibited a trend toward disorder while *Crem* high TAM samples did not. This is of particular interest, as we have observed that acidic pH can enhance circadian rhythms in macrophages, raising the question of whether acidic pH promotes or protects against circadian disorder. We have shown that various stimuli can alter rhythms of macrophages in a complex and contributing manner, including polarizing stimuli, acidic pH, and lactate. TGFβ is produced by a variety of cells within the TME, and was recently identified as a signal that can modulate circadian rhythms (Finger et al, 2021; Massagué, 2008). In addition, when we exposed macrophages to cancer cell-conditioned media, rhythms were modulated in a manner distinct from acidic pH or lactate, with these changes in rhythms partially reversed by neutralization of the cancer cell-conditioned media pH (Fig. EV3). It is conceivable that, in addition to acidic pH, other stimuli in the TME are influencing circadian rhythms to drive population-level disorder that we observed by CCD.

Supporting the notion that population-level disorder may exist in TAMs, we used scRNA-sequencing data and found evidence of heterogeneity between the expression of circadian clock genes in different TAM subpopulations (Fig. 9A,B). Phenotypic heterogeneity of TAMs in various types of cancer has previously been shown (Chevrier et al, 2017; Lavin et al, 2017; Laviron et al, 2022; Storrs et al, 2023), and we have identified distinct TAM subpopulations by unbiased clustering (Fig. 9A). Within those TAM subpopulations, we identified differential expression of circadian clock genes encoding transcription factors that bind to different consensus sequences (Fig. 9B): DEC1 and DEC2 bind to E-boxes, NFIL3 and DBP binds to D-boxes, and RORα and REV-ERBβ binds to retinoic acid-related orphan receptor elements (ROREs) (Kato et al, 2014; Takahashi, 2017). While little is known about regulation of macrophages by D-box elements beyond the

circadian clock, aspects of macrophage function have been shown to be subject to transcriptional regulation through RORE- and E-box-binding transcription factors (Billon et al, 2019; Pastore et al, 2016; Pello et al, 2012; Rehli et al, 2005; Sato et al, 2014). Thus, we speculate that variations in the circadian transcription factors that were identified to be differentially expressed between TAM subpopulations (Fig. 9B) may exert influence on expression of genes to drive diversity within the TAM population. Differential expression of circadian clock genes between TAM subpopulations was also associated with *Crem* expression (Fig. 9C–E), suggesting that exposure of TAMs to acidic pH within the TME can alter the circadian clock. However, there remained significant variation in expression of circadian clock genes within the *Crem* high and *Crem* low groups (Fig. 9B), suggesting that acidic pH is not the only factor in the TME that can alter the circadian clock. Together, these data implicate the TME in driving heterogeneity in TAM circadian rhythms just as it drives heterogeneity in TAM phenotype.

Interestingly, in contrast to our observations of circadian disorder in TAMs isolated from LLC tumors (Fig. 6), rhythmicity in expression of circadian genes was observed in bulk TAMs isolated from B16 tumors (Wang et al, 2024b). This suggests that circadian rhythms of TAMs are maintained differently in different types of cancer. Notably, both of these observations were at the population level. Upon separation of the B16 TAM population into subsets by unbiased clustering of single-cell RNA-sequencing data, we measured differences in expression of circadian clock genes between TAM subpopulations (Fig. 9A,B). This suggests that even within a rhythmic TAM population, there is heterogeneity in the circadian clock of TAM subpopulations.

Considering our observations that conditions associated with the TME can alter circadian rhythms in macrophages, it becomes increasingly important to understand the relevance of macrophage rhythms to their function in tumors. It has been shown that acidic pH and lactate can each drive functional polarization of macrophages toward a phenotype that promotes tumor growth, with acidic pH modulating phagocytosis and suppressing inflammatory cytokine secretion and cytotoxicity (Colegio et al, 2014; El-Kenawi et al, 2019; Jiang et al, 2021b). However, how the changes in circadian rhythms of macrophages driven by these conditions contributes to their altered function remains unknown. Current evidence suggests that circadian rhythms confer a time-of-day-dependency on macrophage function by gating the macrophage response to inflammatory stimuli based on time-of-day. As such, responses to inflammatory stimuli such as LPS or bacteria are heightened during the active phase while the inflammatory response is suppressed during the inactive phase. An important future direction will be to determine how changes in circadian rhythms of macrophages, such as those observed under acidic pH or high lactate, influences the circadian gating of their function. Data from our lab and others suggest that disruption of the macrophage-intrinsic circadian clock accelerates tumor growth, indicating that circadian regulation of macrophages is tumor-suppressive in models of PDAC (Fig. 10) and melanoma (Alexander et al, 2020). This agrees with complementary findings that behavioral disruption of circadian rhythms in mice (through chronic jetlag) disrupts tumor macrophage circadian rhythms and accelerates tumor growth (Aiello et al, 2020). It remains unclear whether this is through pro-tumorigenic functions of macrophages such as extracellular matrix remodeling or angiogenesis, through suppression of the anti-tumor immune response, or a combination of both functions. Further work will be needed to tease apart these distinctions.

Whereas much work has been done to characterize how macrophages are regulated within the TME, the impact of the TME on circadian rhythms of macrophages remained elusive. Our work uncovers a novel way in which conditions associated with the TME can influence macrophage biology through modulation of circadian rhythms. While the majority of studies investigating the circadian regulation of macrophages have been conducted studying macrophages under homeostatic conditions or in response to acute inflammation (Geiger et al, 2019; Gibbs et al, 2012; Keller et al, 2009; Kitchen et al, 2020; Nguyen et al, 2013), our work contributes to an emerging body of evidence that the tissue microenvironment can influence circadian rhythms (Finger et al, 2021). This is increasingly important when considering the role of circadian rhythms in immune responses at sites of ongoing, chronic inflammation where the microenvironment is altered, such as within tumors. In identifying factors within the TME that can modulate circadian rhythms of macrophages and uncovering evidence of circadian disorder within tumor-associated macrophages, our work lays the foundation for further studies aimed at understanding how the TME can influence the function of tumor-associated macrophages through modulation of circadian rhythms.

Limitations of the study

Our observations of rhythms in macrophages of different phenotypes are limited by in vitro polarization models. It is important to note that while our data suggest that pro-inflammatory macrophages have suppressed rhythms and increased rate of desynchrony, it remains unclear the extent to which these findings apply to the range of pro-inflammatory macrophages found in vivo. We use IFNγ and LPS co-treatment in vitro to model a pro-inflammatory macrophage phenotype that is commonly referred to as 'M1', but under inflammatory conditions in vivo, macrophages are exposed to a variety of stimuli that result in a spectrum of phenotypes, each highly context-dependent. The same is true for 'M2'; different tissue microenvironment are different and pro-resolution macrophages exist in a spectrum. Rhythms were heavily suppressed in pro-inflammatory macrophages, which made analysis of rhythm parameters in pro-inflammatory macrophages more challenging as amplitude and signal reached limit of detection. Our observations of changes in amplitude and period in pro-inflammatory macrophages compared to unstimulated macrophages agrees with the literature, where these changes in rhythms have been observed using LumiCycle as well as by mRNA (Chen et al, 2020; Lellupitiyage Don et al, 2022). This supports the validity and reproducibility of our observations despite the challenges of observing and analyzing rhythms of pro-inflammatory macrophages.

Methods

Reagents and tools table

Reagent/Resource	Reference or Source	Identifier or Catalog Number
Experimental Models		
LysM-cre mice on C57B6 background	Jackson Labs	Strain # 004781
Bmal1^flox/flox mice on C57B6 background	Jackson Labs	Strain # 007668
PER2-Luciferase mice on C57B6 background	Jackson Labs	Strain # 006852

Reagent/Resource	Reference or Source	Identifier or Catalog Number
KCKO Pancreatic cancer mouse cells from C57B6 strain P48-Cre; LSL-KRAS^G12D; Muc1KO	(Besmer et al, 2011)	Not commercially available
L929 mouse cell line	ATCC	CAT#CCL-1
Recombinant DNA		
N/A		
Antibodies		
Rabbit anti-p-CREB (Ser133, Ser129)	Invitrogen	CAT#44-297G
Goat anti-rabbit Alexa Fluor 680	Invitrogen	CAT#A21109
Oligonucleotides and other sequence-based reagents		

qPCR primer name	Source and/or Catalog Number	Primer Sequences
Arg1	(Liu et al, 2017)	5'-CTCCAAGCCAAAGTCCTTAGAG-3', 5'-AGGAGCTGTCATTAGGGACATC-3'
Chil3	IDT Mm.PT.58.33370435	5'-AGAAGCAATCCTGAAGACACC-3', 5'-ACTGGTATAGTAGCACATCAGC-3'
Clec10a	IDT Mm.PT.56a.19092703	5'-TGACTGAGTTCCTGCCTCT-3', 5'-GACCAAGGAGAGTGCTAGAAG-3'
Cry1	(Huber et al, 2016a)	5'-GCTATGCTCCTGGAGAGAACG T-3', 5'-TGTCCCCGTGAGCATAGTGTAA-3'
Icer	(Bohn et al, 2018)	5'-ATGGCTGTAACTGGAGATGAA-3', 5'-GTGGCAAAGCAGTAGTAGGA-3'
Il1b	(Liu et al, 2017)	5'-TACGGACCCCAAAAGATGA-3', 5'-TGCTGCTGCGAGATTTGAAG-3'
Il6	(Liu et al, 2017)	5'-TAGTCCTTCCTACCCCAATTTCC-3', 5'-TTGGTCCTTAGCCACTCCTTC-3'
Mrc1	IDT Mm.PT.58.42560062	5'-CAAGTTGCCGTCTGAACTGA-3', 5'-TATCTCTGTCATCCCTGTCTCT-3'
Nos2	IDT Mm.PT.58.43705194	5'-GCTTCTGGTCGATGTCATGAG-3', 5'-TCCACCAGGAGATGTTGAAC-3'
Nr1d1	IDT Mm.PT.58.17472803	5'-GAGCCACTAGAGCCAATGTAG-3', 5'-CCAGTTTGAATGACCGCTTTC-3'
Per2	IDT Mm.PT.58.5594166	5'-TGAGGTAGATAGCCCAGGAG-3', 5'-GCTATGAAGCGCCTAGAATCC-3'
Retnla	(Liu et al, 2017)	5'-CTGGGTTCTCCACCTCTTCA-3', 5'-TGCTGGGATGACTGCTACTG-3'
Tbp	IDT Mm.PT.39a.22214839	5'-CCAGAACTGAAAATCAACGCAG-3', 5'-TGTATCTACCGTGAATCTTGGC-3'
Tnfa	(Liu et al, 2017)	5'-ACGGCATGGATCTCAAAGAC-3', 5'-AGATAGCAAATCGGCTGACG-3'
Vegf	(Colegio et al, 2014)	5'-CCACGACAGAAGGAGAGCAGAAGTCC-3', 5'-CGTTACAGCAGCCTGCACAGCG-3'
Chemicals, Enzymes and other reagents		
RPMI media	Corning	CAT#MT10040CV
RPMI powdered media	Corning	CAT#50-020-PC
Low endotoxin fetal bovine serum	Cytiva	CAT#SH30396.03
Penicillin-Streptomycin	Gibco	CAT# 15140122
Horse serum	Corning	CAT#35030CV
HEPES	Gibco	CAT#15630080
PIPES	Sigma	CAT#P1851
NaOH	EMD Millipore	CAT#SX0593-1
Mouse IL-4 recombinant protein	Thermo/Peprotech	CAT#214-14
Mouse IL-13 recombinant protein	Thermo/Peprotech	CAT#210-13
Mouse IFNγ recombinant protein	Thermo/Peprotech	CAT#315-05
Lipopolysaccharide (LPS)	Invitrogen	CAT#00497693
Sodium-L-lactate	Sigma	CAT#L7022
MDL-12330A	Sigma	CAT#M182
3-Isobutyl-1-methylxanthine (IBMX)	Sigma	CAT#I5879

Reagent/Resource	Reference or Source	Identifier or Catalog Number
Forskolin	Sigma	CAT#344270
Beetle D-luciferin	Promega	CAT#E1602
Oligo d(T)16	Invitrogen	CAT#N8080128
PerfeCTa SYBR Green FastMix	QuantBio	CAT#95074-05K
M-Per lysis reagent	Thermo Scientific	CAT#78501
Protease and phosphatase inhibitor cocktail	Sigma	CAT#PPC1010
Phosphatase inhibitor cocktail 2	Sigma	CAT#D9533
Hoechst Nucleic Acid Stain	Thermo Scientific	CAT#62249
Isoflurane (Fluriso™)	VetOne Fluriso	CAT#501017
Normal Saline 0.9%	Medline	CAT#RDI30296
Software		
Ubuntu v18.04	Microsoft Store	
Bioconda v23.1.0	https://bioconda.github.io/	
R v3.6.3 or v4.0.5	https://cran.r-project.org/	
R Studio v2024.04.2	https://posit.co/	
GraphPad Prism v10.3.0	https://www.graphpad.com/	
Other		
EZNA HP Total RNA Kit	Omega Biotek	CAT#R6812-02
Taqman Reverse Transcription Reagents	Invitrogen	CAT#N8080234
QuantStudio 5 384-well qPCR machine	Applied Biosystems	CAT#A28140
Bio-Rad DC Protein Assay Kit	Bio-Rad	CAT#5000112
Bio-Rad Criterion 4–15% Criterion TGX Stain-Free 26-well gradient gel	Bio-Rad	CAT#5678095
TransBlot Turbo Tranfer System	Bio-Rad	CAT#1704150
Trans-Blot Turbo RTA Midi 0.2 μm Nitrocellulose Transfer Kit	Bio-Rad	Bio-Rad CAT#1704271

Animals

Mice were maintained in individually ventilated cages with bedding and nesting material in a temperature-controlled, pathogen-free environment in the animal care facility at the University of Rochester. All animal protocols were approved by the University of Rochester Committee of Animal Resources (UCAR, approval #UCAR-2019-014). The University of Rochester Medical Center Animal Facility is fully accredited by AAALAC International and in compliance with state law, federal statute and NIH policy. All experiments were performed in compliance with the NIH- and University of Rochester-approved guidelines for the use and care of animals, as well as recommendations in the Guide for the Care and Use of Laboratory Animals of the National Research Council (Committee, 2011). Mice were housed on a 12:12 light dark cycle. In some cases, to ease timepoint collection, mice were housed under reverse lighting conditions in a 12:12 dark light cycle for at least 2 weeks prior to use in experiments. Mice used for experiments were between the ages of 8–14 weeks old; both male and female mice were used. Mice were euthanized humanely prior to harvesting peritoneal macrophages or bone marrow.

Previously characterized mice with a myeloid-specific deletion of BMAL1 (LysM-cre$^{+/-}$Bmal1$^{flox/flox}$; referred to as BMAL1 KO mice) (Gibbs et al, 2012) in a C57BL/6 background were generated by crossing LysM-cre mice (Clausen et al, 1999) with Bmal1$^{flox/flox}$ mice (Storch et al, 2007). These mice were further crossed with PER2-Luc mice (Yoo et al, 2004) to generate BMAL1 KO or wild-type control mice (LysM-cre$^{-/-}$Bmal1$^{flox/flox}$; referred to as WT) expressing PER2-Luc. PER2-Luc (strain #006852), LysM-cre (strain #004781), and Bmal1$^{flox/flox}$ (strain #007668) mice used for breeding to generate WT and BMAL1 KO mice were purchased from the Jackson Laboratory.

Differentiation and culture of bone marrow-derived macrophages

Bone marrow-derived macrophages (BMDMs) were generated from bone marrow isolated from WT mice using a well-established protocol for differentiation of BMDMs over 7 days (Gonçalves and Mosser, 2015; Trouplin et al, 2013). In brief, bone marrow cells were seeded at 200,000 cells/mL on non-tissue culture treated-plates in BMDM Differentiation Media: RPMI (Corning, CAT#MT10040CV) supplemented with 20% (v/v) L929 supernatant, 10% (v/v) heat-inactivated (HI) fetal bovine serum (FBS) (Cytiva, CAT#SH30396.03), and 100 U/mL Penicillin-Streptomycin (Gibco, CAT# 15140122). Cells were grown at 37 °C in air enriched with 5% CO_2. On day 3, additional BMDM Differentiation Media was added to cells. On day 6 of the differentiation protocol, BMDMs were seeded at 1.2×10^6 cells/mL and left in BMDM Differentiation Media, and kept at 37 °C in air enriched with 5% CO_2. On day 7, BMDM Differentiation Media was removed and BMDMs were synchronized.

To synchronize BMDMs, we adapted a recently published method (Collins et al, 2021). Briefly, BMDMs were first serum starved for 24 h in serum-free media (RPMI, supplemented with 100 U/mL Penicillin-Streptomycin); BMDMs were then subjected to serum shock by replacing serum-free media with RPMI supplemented with 50% (v/V) HI horse serum (Corning, CAT#35030CV) at 37 °C in air enriched with 5% CO_2. At the end of this synchronization protocol, media was replaced with Atmospheric Media, which has been formulated for use at atmospheric CO_2 levels and enhanced pH stability by increasing buffering capacity at low pH (Walton et al, 2018): RPMI (Corning, CAT#50-020-PC), 25 mM HEPES (Gibco, CAT#15630080), 25 mM PIPES (Sigma, CAT#P1851), supplemented with 10% (v/v) HI FBS and 100 U/mL Penicillin-Streptomycin (Walton et al, 2018). Atmospheric Media was adjusted to pH 7.4, 6.8, or 6.5 with NaOH (EMD Millipore CAT#SX0593-1) and filter-sterilized.

BMDMs cultured in Atmospheric Media at pH 7.4, 6.8, or 6.5 were either left unstimulated or were polarized toward a pro-resolution ('M2') or pro-inflammatory phenotype ('M1') by addition of 10 ng/mL IL-4 (PeproTech, CAT#214-14) and 10 ng/mL IL-13 (PeproTech, CAT#210-13), or 50 ng/mL IFNγ (PeproTech, CAT#315-05) and 100 ng/mL LPS (Invitrogen, CAT#00497693), respectively. For lactate experiments, sodium-L-lactate (Sigma, CAT#L7022) or vehicle was added to Atmospheric Media for a final concentration of 25 mM or 0 mM. For interrogation of cAMP signaling pathway, BMDMs were cultured in Atmospheric Media at pH 7.4 or 6.5 with vehicle or 5, 10, or 15 μM MDL-12330A (Sigma, CAT#M182). For phenocopy experiments (Fig. 5; Appendix Fig. S4), BMDMs were not synchronized prior to the experiment. BMDMs were cultured in Atmospheric

Media at pH 7.4 or 6.5 with vehicle or 20, 40, or 80 μM IBMX (Sigma, CAT#I5879) or forskolin (Sigma, CAT#344270). For LumiCycle experiments, 100 mM D-luciferin was added to Atmospheric Media at 1:1000 for 100 μM D-luciferin (Promega, CAT#E1602). Cells cultured in Atmospheric Media were kept at 37 °C in atmospheric conditions and were either monitored over time by LumiCycle or harvested for RNA or protein at the time points indicated.

Isolation and culture of peritoneal macrophages

Peritoneal exudate cells were harvested from mice as previously published (Ray and Dittel, 2010). To isolate peritoneal macrophages, peritoneal exudate cells were seeded at 1.2×10^6 cells/mL in RPMI/10% HI FBS supplemented with 100 U/mL Penicillin-Streptomycin and left at 37 °C for 1 h, after which non-adherent cells were rinsed off (Gonçalves and Mosser, 2015). Isolation of peritoneal macrophages using this method has been shown to yield a population that is over 90% pure macrophages (De Jesus et al, 2022; Layoun et al, 2015). Peritoneal macrophages were then cultured in Atmospheric Media at pH 7.4 or 6.5 with 100 μM D-luciferin and kept at 37 °C in atmospheric conditions.

Quantification of circadian rhythm parameters

Using the Lumicycle Analysis program version 2.701 (Actimetrics), raw data was fitted to a linear baseline, and the baseline-subtracted data was fitted to a damped sine wave from which period and damping were calculated (Ramanathan et al, 2014). Amplitude was calculated from baseline-subtracted data by subtracting the bioluminescent values of the first peak from the first trough as previously published (Chen et al, 2020).

Production of KCKO cancer cell supernatant

KCKO cells were seeded at 300,000 cells/mL in pH 7.4 Atmospheric Media (RPMI buffered for use at atmospheric CO_2 levels and enhanced buffering capacity at low pH—see "Differentiation and culture of bone marrow-derived macrophages" section) and cultured at 37 °C in atmospheric conditions for 5 days. Supernatant was then collected, pH-adjusted to pH 7.4 or 6.5, and filter-sterilized. For the experiment, bone marrow-derived macrophages were cultured in pH 7.4 or pH 6.5 KCKO supernatant, or pH 7.4 or pH 6.5 Atmospheric Media. Media was supplemented with 100 μM D-luciferin, and cells were kept at 37 °C in atmospheric conditions and monitored over time by LumiCycle.

Quantitative PCR

Cells were lysed and RNA was isolated using the E.Z.N.A. HP Total RNA Kit (Omega BioTek, CAT#R6812-02). RNA was reverse transcribed to cDNA using the Taqman Reverse Transcription Reagents system (Invitrogen CAT#N8080234), using oligo dT for priming (Invitrogen CAT#N8080128). qPCR was performed with cDNA using PerfeCTa SYBR Green FastMix (QuantaBio, CAT#95074-05K) and with the Quant Studio 5 quantitative PCR machines (Applied Biosystems). Triplicate technical replicates were performed, outlier replicates (defined as being more than 1 Ct away from other two replicates) were discarded, and relative mRNA was normalized to *Tbp* and assessed by the ΔΔCt. See Reagents and Tools Table for primer sources and sequences.

Immunoblot

Cells were lysed using the M-Per lysis reagent (Thermo Scientific, CAT#78501), supplemented with protease and phosphatase inhibitor cocktail (1:100; Sigma, CAT#PPC1010) and phosphatase inhibitor cocktail 2 (1:50; Sigma, CAT#P5726), with 200 μM deferoxamine (Sigma, CAT#D9533). M-Per is formulated to lyse the nucleus and solubilize nuclear and chromatin-bound proteins, allowing isolation of nuclear proteins as well as cytosolic proteins. Lysates were incubated on ice for 1 h, then centrifuged at $17,000 \times g$ to pellet out debris; supernatant was collected. Protein was quantified using the Bio-Rad DC Protein Assay Kit (Bio-Rad, CAT#5000112), and lysates of equal concentration were prepared and run by SDS-PAGE on Bio-Rad Criterion 4–15% Criterion TGX Stain-Free 26-well gradient gel (Bio-Rad, CAT#5678095). Gels were transferred using the Trans-Blot Turbo system (Bio-Rad CAT#1704150) to nitrocellulose membranes (Bio-Rad CAT#1704271).

The following primary antibody was used: rabbit anti-p-CREB (Ser133, Ser129) (Invitrogen, CAT#44-297G). The following secondary antibody was used: goat anti-rabbit Alexa Fluor 680 (Invitrogen, CAT#A21109). Of note, two different anti-CREB antibodies were tested (Cell Signaling, CAT#9197 and Invitrogen, CAT#35-0900) in combination with appropriate secondary antibodies but neither revealed bands at the correct molecular weight for CREB protein. Membranes were digitally imaged using a ChemiDoc MP (Bio-Rad) and uniformly contrasted. Total protein was imaged by Stain-Free imaging technology (Bio-Rad) and used as loading control. To visualize total protein, image of entire membrane was shrunk to match the size of pCREB.

Survival under acidic pH

BMDMs were seeded, in triplicate, at 1.2×10^6 cells/mL in a 96-well plate. BMDMs were synchronized, then cultured in Atmospheric Media at pH 7.4, 6.8, or 6.5 containing 10 ng/mL IL-4 and 10 ng/mL IL-13, or 50 ng/mL IFNγ and 100 ng/mL LPS, or vehicle for unstimulated control. BMDMs were fixed at 1, 2, and 3 days later. BMDMs were stained with Hoechst (Thermo Scientific, CAT#62249), and plates were imaged using a Celigo S. Number of nuclei per well was enumerated using Celigo software to quantify the number of adherent BMDMs after time in culture under acidic conditions as a readout of survival.

Tumor growth

Mice were anesthetized via inhalation of 4 vol% isoflurane (Fluriso™, VetOne, CAT#501017) in 100% oxygen at a flow rate of 4 L/min prior to injection. Following application of 70% ethanol to the site of injection, with 1×10^6 WT or BMAL1 KO macrophages and 1×10^6 KCKO cells in 100 μL sterile 0.9% normal saline (Medline, CAT#RDI30296) were subcutaneously co-injected in the flank of WT mice. In line with previously published co-injection tumor experiments, mice were injected with macrophages at a 1:1 ratio (Alexander et al, 2020; Colegio et al, 2014). Tumor growth was measured by caliper, and volume was calculated by the modified ellipsoidal formula: tumor volume = $0.5 \times (\text{length} \times \text{width}^2)$ (Tomayko and Reynolds, 1989). When tumors did not engraft and grow, these animals were excluded. Mice were euthanized when there was ulcer formation or when tumor size reached a diameter of 20 mm.

Processing and analysis of publicly available bulk gene expression data

FASTQ files from a previously published analysis of peritoneal macrophages cultured under neutral pH 7.4 or acidic pH 6.8 conditions were downloaded from NCBI GEO (Data ref: accession #GSE164697) (Jiang et al, 2021b, a). FASTQ files from a previously published analysis of peritoneal macrophages from WT or BMAL1 KO mice were downloaded from EMBL- European Bioinformatics Institute Array Express (Data ref: accession #E-MTAB-8411) (Kitchen et al, 2019, 2020). FASTQ files from a previously published analysis of bone marrow-derived macrophages were downloaded from NCBI GEO (Data ref: accession #GSE157878) (Collins et al, 2020, 2021). FASTQ files from a previously published analysis of macrophages from tumor and tumor-adjacent tissue from NSCLC patients were downloaded from NCBI GEO (Data ref: accession #GSE116946) (Garrido-Martin et al, 2020a, b). FASTQ files from a previous published study of tumor-associated macrophages were downloaded from NCBI GEO (Data ref: accession #GSE188549) (Geeraerts et al, 2021a, b). Where applicable, multiple FASTQ files of the same run were concatenated before processing and mapping. CEL files from a previously published microarray time series analysis of peritoneal macrophages from WT mice were downloaded from NCBI GEO (Data ref: accession #GSE25585) (Keller et al, 2009, 2010). CEL files from a previously published microarray analysis of alveolar macrophages from healthy human donors were downloaded from NCBI GEO (Data ref: accession #GSE13896) (Shaykhiev et al, 2009a, b).

All FASTQ files were processed with FASTP using default parameters to trim adapters and remove reads that were low quality or too short (Chen et al, 2018). Cleaned FASTQ files from mouse data were mapped to transcripts using Salmon 1.4.0 in mapping-based mode using a decoy-aware transcription built from the Gencode M27 GRCm39 primary assembly mouse genome and M27 mouse transcriptome, and from human data were mapped to transcripts using Salmon v1.4.0 in mapping-based mode using a decoy-aware transcription built from the Gencode v43 GRCh38 primary assembly human genome and v43 human transcriptome (Patro et al, 2017). Single-end mapping was used for GSE188549, GSE116946 samples and paired-end mapping was used for E-MTAB-8411 and GSE164697. All transcripts were then collapsed to gene-level using Tximport v1.14.2 with the Gencode M27 transcriptome for mouse and the v43 transcriptome for human, and genes were annotated with symbols using the Ensembl GRCm39.104 transcriptome annotations for mouse and Ensembl GRCh38.111 transcriptome annotations for human (Soneson et al, 2015). Transcripts per million (TPM) outputted from Tximport were used for downstream analyses. Microarray data was imported and analyzed from CEL files using the packages affy v1.68.0 and Limma v3.46.0, and genes were annotated with symbols using the University of Michigan Brain Array Custom CDF v25.0 for the Mouse Gene 1.0 ST Array or Human Gene 133 plus 2 Array (Dai et al, 2005; Ritchie et al, 2015).

Clock correlation distance (CCD) analysis was performed as previously described (Shilts et al, 2018), using v1.0.4. Briefly, the default universal 12-gene molecular circadian clock reference correlation was used. Genes outside this 12-gene reference that were of zero variance across at least one of the sample groups were discarded prior to analysis. For delta CCD, which directly compares between each group, the sample group with the lowest CCD score (corresponding to the most ordered clock) was set as the control group, and $p < 0.05$ was deemed significantly different from the control group. DeltaCCD determines significance by permuting the sample labels 1000 times, keeping the reference sample group the same, and uses the method of Phipson and Smith to determine an exact one-sided p value.

WCGNA v1.72-5 analysis to determine significant covariance between pairs of clock genes was performed as previously described, using an expanded list of core circadian clock genes (Geeraerts et al, 2021a). Results were calculated from Pearson correlations of log-transformed TPM values. For data presented in Fig. 6, the gene-specific mean for TAMs within each group in the original publication (MHCII-high and MHCII-low, (Geeraerts et al, 2021a, b)) were subtracted out prior to analysis. Significance was determined by $p < 0.05$ (Fig. 6) or $p < 0.01$ (Figs. 7 and EV5). Note that WGCNA does not output exact P values.

Processing and analysis of publicly available single-cell gene expression data

A merged Seurat Object of single-cell RNA-sequencing data of immune cells infiltrating B16-F10 melanoma was downloaded from NCBI GEO (Data ref: accession #GSE260641) (Wang et al, 2024a, b). Data were analyzed using Seurat 5.0.3 (Butler et al, 2018). Macrophages, which were previously annotated, were isolated, gene expression normalized, and the following factors regressed out: cell cycle state, mitochondrial content, and circadian timepoint. 9 clusters were identified with the FindNeighbors and FindClusters commands. UMAP was used to visualize macrophage clusters (Becht et al, 2019). *Crem* high groups were identified from violin plot and confirmed with differential expression compared to *Crem* low groups. All differential expression was performed using the FindMarkers command only considering genes expressed within at least 10% of the comparison populations and with a minimum log fold change of 0.25 between populations (min.pct = 0.1 and logfc.theshold = 0.25). Significantly differentially expressed genes were determined by adjusted p(adj.p) < 0.05 by the limma implementation of the Wilcoxon Rank-Sum test (test.use = "wilcox_limma") (Ritchie et al, 2015; Smyth, 2005). A differentially expressed genes shown are p(adj.p) < 0.005.

Software

Analyses in the Windows BASH Shell were run using Ubuntu version 18.04 and Bioconda version 23.1.0. Analyses in R were run using R versions 3.6.3 or 4.0.5 in R Studio version 2024.04.2. Analyses in GraphPad Prism were run using GraphPad Prism 10.3.0.

Power calculations and blinding

Sample sizes were determined from power calculations using data from small pilot experiments. Researchers were not blinded to conditions, but were blinded to results while taking measurements. For tumor assays, tumor measurements were not graphed and analyzed until after completion of experiment.

Graphics

The following Figures were created using Biorender.com: Fig. 8A, Fig. 10C, Fig. EV1A, and the Summary Figure.

Data availability

All raw data, analyses, and code used for analyses are available at FigShare at the following link: https://rochester.figshare.com/projects/Source_data_for_Circadian_rhythms_of_macrophages_are_altered_by_the_acidic_pH_of_the_tumor_microenvironment/210625.

The source data of this paper are collected in the following database record: biostudies:S-SCDT-10_1038-S44319-024-00288-2.

Expanded view data, supplementary information, appendices are available for this paper at https://doi.org/10.1038/s44319-024-00288-2.

Peer review information

A peer review file is available at https://doi.org/10.1038/s44319-024-00288-2

References

Abe M, Herzog ED, Yamazaki S, Straume M, Tei H, Sakaki Y, Menaker M, Block GD (2002) Circadian rhythms in isolated brain regions. J Neurosci 22:350–356

Adrover JM, Del Fresno C, Crainiciuc G, Cuartero MI, Casanova-Acebes M, Weiss LA, Huerga-Encabo H, Silvestre-Roig C, Rossaint J, Cossio I et al (2019) A neutrophil timer coordinates immune defense and vascular protection. Immunity 50:390–402.e310

Aiello I, Fedele MLM, Román F, Marpegan L, Caldart C, Chiesa JJ, Golombek DA, Finkielstein CV, Paladino N (2020) Circadian disruption promotes tumor-immune microenvironment remodeling favoring tumor cell proliferation. Sci Adv 6:eaaz4530

Alexander RK, Liou Y-H, Knudsen NH, Starost KA, Xu C, Hyde AL, Liu S, Jacobi D, Liao N-S, Lee C-H (2020) Bmal1 integrates mitochondrial metabolism and macrophage activation. eLife 9:e54090

Allen JE (2023) IL-4 and IL-13: regulators and effectors of wound repair. Annu Rev Immunol 41:229–254

Arjona A, Sarkar DK (2005) Circadian oscillations of clock genes, cytolytic factors, and cytokines in rat NK cells. J Immunol (Baltim, Md: 1950) 174:7618–7624

Baumann A, Gönnenwein S, Bischoff SC, Sherman H, Chapnik N, Froy O, Lorentz A (2013) The circadian clock is functional in eosinophils and mast cells. Immunology 140:465–474

Beam CA, Wasserfall C, Woodwyk A, Akers M, Rauch H, Blok T, Mason P, Vos D, Perry D, Brusko T et al (2020) Synchronization of the normal human peripheral immune system: a comprehensive circadian systems immunology analysis. Sci Rep 10:672

Becht E, McInnes L, Healy J, Dutertre C-A, Kwok IWH, Ng LG, Ginhoux F, Newell EW (2019) Dimensionality reduction for visualizing single-cell data using UMAP. Nat Biotechnol 37:38–44

Besmer DM, Curry JM, Roy LD, Tinder TL, Sahraei M, Schettini J, Hwang SI, Lee YY, Gendler SJ, Mukherjee P (2011) Pancreatic ductal adenocarcinoma mice lacking mucin 1 have a profound defect in tumor growth and metastasis. Cancer Res 71:4432–4442

Billon C, Murray MH, Avdagic A, Burris TP (2019) RORγ regulates the NLRP3 inflammasome. J Biol Chem 294:10–19

Binger KJ, Gebhardt M, Heinig M, Rintisch C, Schroeder A, Neuhofer W, Hilgers K, Manzel A, Schwartz C, Kleinewietfeld M et al (2015) High salt reduces the activation of IL-4- and IL-13-stimulated macrophages. J Clin Investig 125:4223–4238

Biswas SK, Gangi L, Paul S, Schioppa T, Saccani A, Sironi M, Bottazzi B, Doni A, Vincenzo B, Pasqualini F et al (2006) A distinct and unique transcriptional program expressed by tumor-associated macrophages (defective NF-kappaB and enhanced IRF-3/STAT1 activation). Blood 107:2112–2122

Biswas SK, Mantovani A (2010) Macrophage plasticity and interaction with lymphocyte subsets: cancer as a paradigm. Nat Immunol 11:889–896

Boedtkjer E, Pedersen SF (2020) The acidic tumor microenvironment as a driver of cancer. Annu Rev Physiol 82:103–126

Bohn T, Rapp S, Luther N, Klein M, Bruehl TJ, Kojima N, Aranda Lopez P, Hahlbrock J, Muth S, Endo S et al (2018) Tumor immunoevasion via acidosis-dependent induction of regulatory tumor-associated macrophages. Nat Immunol 19:1319–1329

Butler A, Hoffman P, Smibert P, Papalexi E, Satija R (2018) Integrating single-cell transcriptomic data across different conditions, technologies, and species. Nat Biotechnol 36:411–420

Cassetta L, Pollard JW (2018) Targeting macrophages: therapeutic approaches in cancer. Nat Rev Drug Discov 17:887–904

Certo M, Llibre A, Lee W, Mauro C (2022) Understanding lactate sensing and signalling. Trends Endocrinol Metab: TEM 33:722–735

Chen S, Fuller KK, Dunlap JC, Loros JJ (2020) A pro- and anti-inflammatory axis modulates the macrophage circadian clock. Front Immunol 11:867

Chen S, Zhou Y, Chen Y, Gu J (2018) fastp: an ultra-fast all-in-one FASTQ preprocessor. Bioinformatics 34:i884–i890

Chevrier S, Levine JH, Zanotelli VRT, Silina K, Schulz D, Bacac M, Ries CH, Ailles L, Jewett MAS, Moch H et al (2017) An immune atlas of clear cell renal cell carcinoma. Cell 169:736–749.e718

Chun SK, Fortin BM, Fellows RC, Habowski AN, Verlande A, Song WA, Mahieu AL, Lefebvre A, Sterrenberg JN, Velez LM et al (2022) Disruption of the circadian clock drives Apc loss of heterozygosity to accelerate colorectal cancer. Sci Adv 8:eabo2389

Clausen BE, Burkhardt C, Reith W, Renkawitz R, Förster I (1999) Conditional gene targeting in macrophages and granulocytes using LysMcre mice. Transgenic Res 8:265–277

Colegio OR, Chu NQ, Szabo AL, Chu T, Rhebergen AM, Jairam V, Cyrus N, Brokowski CE, Eisenbarth SC, Phillips GM et al (2014) Functional polarization of tumour-associated macrophages by tumour-derived lactic acid. Nature 513:559–563

Collins EJ, Cervantes-Silva MP, Timmons GA, O'Siorain JR, Curtis AM, Hurley JM (2020) Circadian profiling of the bone marrow derived macrophage transcriptome. GSE157878 [DATASET]

Collins EJ, Cervantes-Silva MP, Timmons GA, O'Siorain JR, Curtis AM, Hurley JM (2021) Post-transcriptional circadian regulation in macrophages organizes temporally distinct immunometabolic states. Genome Res 31:171–185

Committee NRC (2011) Guide for the care and use of laboratory animals. National Academies Press (US), Washington (DC) https://www.ncbi.nlm.nih.gov/books/NBK54050/

Cook RS, Jacobsen KM, Wofford AM, DeRyckere D, Stanford J, Prieto AL, Redente E, Sandahl M, Hunter DM, Strunk KE et al (2013) MerTK inhibition in tumor leukocytes decreases tumor growth and metastasis. J Clin Investig 123:3231–3242

Coussens LM, Werb Z (2002) Inflammation and cancer. Nature 420:860–867

Cuccarese MF, Dubach JM, Pfirschke C, Engblom C, Garris C, Miller MA, Pittet MJ, Weissleder R (2017) Heterogeneity of macrophage infiltration and therapeutic response in lung carcinoma revealed by 3D organ imaging. Nat Commun 8:14293

Curtis AM, Fagundes CT, Yang G, Palsson-McDermott EM, Wochal P, McGettrick AF, Foley NH, Early JO, Chen L, Zhang H et al (2015) Circadian control of innate immunity in macrophages by miR-155 targeting Bmal1. Proc Natl Acad Sci USA 112:7231–7236

Dai M, Wang P, Boyd AD, Kostov G, Athey B, Jones EG, Bunney WE, Myers RM, Speed TP, Akil H et al (2005) Evolving gene/transcript definitions significantly alter the interpretation of GeneChip data. Nucleic acids Res 33:e175

Daniel B, Nagy G, Czimmerer Z, Horvath A, Hammers DW, Cuaranta-Monroy I, Poliska S, Tzerpos P, Kolostyak Z, Hays TT et al (2018) The nuclear receptor PPARγ controls progressive macrophage polarization as a ligand-insensitive epigenomic ratchet of transcriptional memory. Immunity 49:615–626.e616

De Jesus A, Pusec CM, Nguyen T, Keyhani-Nejad F, Gao P, Weinberg SE, Ardehali H (2022) Optimized protocol to isolate primary mouse peritoneal macrophage metabolites. STAR Protoc 3:101668

de la Cruz-López KG, Castro-Muñoz LJ, Reyes-Hernández DO, García-Carrancá A, Manzo-Merino J (2019) Lactate in the regulation of tumor microenvironment and therapeutic approaches. Front Oncol 9:1143

DeNardo DG, Ruffell B (2019) Macrophages as regulators of tumour immunity and immunotherapy. Nat Rev Immunol 19(6):369–382

Deng W, Zhu S, Zeng L, Liu J, Kang R, Yang M, Cao L, Wang H, Billiar TR, Jiang J et al (2018) The circadian clock controls immune checkpoint pathway in sepsis. Cell Rep 24:366–378

Ding C, Sun X, Wu C, Hu X, Zhang HG, Yan J (2019) Tumor microenvironment modulates immunological outcomes of myeloid cells with mTORC1 disruption. J Immunol 202:1623–1634

Druzd D, Matveeva O, Ince L, Harrison U, He W, Schmal C, Herzel H, Tsang AH, Kawakami N, Leliavski A et al (2017) Lymphocyte circadian clocks control lymph node trafficking and adaptive immune responses. Immunity 46:120–132

El-Kenawi A, Gatenbee C, Robertson-Tessi M, Bravo R, Dhillon J, Balagurunathan Y, Berglund A, Vishvakarma N, Ibrahim-Hashim A, Choi J et al (2019) Acidity promotes tumour progression by altering macrophage phenotype in prostate cancer. Br J Cancer 121:556–566

Estrella V, Chen T, Lloyd M, Wojtkowiak J, Cornnell HH, Ibrahim-Hashim A, Bailey K, Balagurunathan Y, Rothberg JM, Sloane BF et al (2013) Acidity generated by the tumor microenvironment drives local invasion. Cancer Res 73:1524–1535

Fadok VA, Bratton DL, Konowal A, Freed PW, Westcott JY, Henson PM (1998) Macrophages that have ingested apoptotic cells in vitro inhibit proinflammatory cytokine production through autocrine/paracrine mechanisms involving TGF-beta, PGE2, and PAF. J Clin Investig 101:890–898

Finger AM, Jäschke S, Del Olmo M, Hurwitz R, Granada AE, Herzel H, Kramer A (2021) Intercellular coupling between peripheral circadian oscillators by TGF-β signaling. Sci Adv 7:eabg5174

Fortier EE, Rooney J, Dardente H, Hardy MP, Labrecque N, Cermakian N (2011) Circadian variation of the response of T cells to antigen. J Immunol 187:6291–6300

Garrido-Martin EM, Mellows TWP, Clarke J, Ganesan AP, Wood O, Cazaly A, Seumois G, Chee SJ, Alzetani A, King EV et al (2020a) M1(hot) tumor-associated macrophages boost tissue-resident memory T cells infiltration and survival in human lung cancer. J Immunother Cancer 8:e000778

Garrido-Martin EM, Mellows TWP, Clarke J, Ganesan AP, Wood O, Cazaly A, Seumois G, Chee SJ, Alzetani A, King EV et al (2020b) M1hot tumour associated macrophages are positively associated with tissue-resident memory T cell responses and survival outcomes in human lung cancer (bulk). GSE116946 [DATASET]

Gaspar LS, Álvaro AR, Carmo-Silva S, Mendes AF, Relógio A, Cavadas C (2019) The importance of determining circadian parameters in pharmacological studies. Br J Pharmacol 176:2827–2847

Gautier EL, Chow A, Spanbroek R, Marcelin G, Greter M, Jakubzick C, Bogunovic M, Leboeuf M, van Rooijen N, Habenicht AJ et al (2012) Systemic analysis of PPARγ in mouse macrophage populations reveals marked diversity in

expression with critical roles in resolution of inflammation and airway immunity. J Immunol 189:2614–2624

Geeraerts X, Fernández-Garcia J, Hartmann FJ, de Goede KE, Martens L, Elkrim Y, Debraekeleer A, Stijlemans B, Vandekeere A, Rinaldi G et al (2021a) Macrophages are metabolically heterogeneous within the tumor microenvironment. Cell Rep 37:110171

Geeraerts X, Fernández-Garcia J, Hartmann FJ, de Goede KE, Martens L, Elkrim Y, Debraekeleer A, Stijlemans B, Vandekeere A, Rinaldi G et al (2021b) Macrophages are metabolically heterogenous within the tumor microenvironment. GSE188549 [DATASET]

Geiger SS, Curtis AM, O'Neill LAJ, Siegel RM (2019) Daily variation in macrophage phagocytosis is clock-independent and dispensable for cytokine production. Immunology 157(2):122–136

Gentles AJ, Newman AM, Liu CL, Bratman SV, Feng W, Kim D, Nair VS, Xu Y, Khuong A, Hoang CD et al (2015) The prognostic landscape of genes and infiltrating immune cells across human cancers. Nat Med 21:938–945

Gibbs JE, Blaikley J, Beesley S, Matthews L, Simpson KD, Boyce SH, Farrow SN, Else KJ, Singh D, Ray DW et al (2012) The nuclear receptor REV-ERBalpha mediates circadian regulation of innate immunity through selective regulation of inflammatory cytokines. Proc Natl Acad Sci USA 109:582–587

Gillies RJ, Liu Z, Bhujwalla Z (1994) 31P-MRS measurements of extracellular pH of tumors using 3-aminopropylphosphonate. Am J Physiol 267:C195–203

Gillies RJ, Pilot C, Marunaka Y, Fais S (2019) Targeting acidity in cancer and diabetes. Biochim Biophys Acta Rev Cancer 1871:273–280

Gonçalves R, Mosser DM (2015) The isolation and characterization of murine macrophages. Curr Protoc Immunol 111:14.11.11–14.11.16

Graham DK, DeRyckere D, Davies KD, Earp HS (2014) The TAM family: phosphatidylserine sensing receptor tyrosine kinases gone awry in cancer. Nat Rev Cancer 14:769–785

Guellaen G, Mahu JL, Mavier P, Berthelot P, Hanoune J (1977) RMI 12330 A, an inhibitor of adenylate cyclase in rat liver. Biochim Biophys Acta 484:465–475

Haspel JA, Anafi R, Brown MK, Cermakian N, Depner C, Desplats P, Gelman AE, Haack M, Jelic S, Kim BS et al (2020) Perfect timing: circadian rhythms, sleep, and immunity—an NIH workshop summary. JCI Insight 5:e131487

He W, Holtkamp S, Hergenhan SM, Kraus K, de Juan A, Weber J, Bradfield P, Grenier JMP, Pelletier J, Druzd D et al (2018) Circadian expression of migratory factors establishes lineage-specific signatures that guide the homing of leukocyte subsets to tissues. Immunity 49:1175–1190.e1177

Hörhold F, Eisel D, Oswald M, Kolte A, Röll D, Osen W, Eichmüller SB, König R (2020) Reprogramming of macrophages employing gene regulatory and metabolic network models. PLOS Comput Biol 16:e1007657

Huang YK, Wang M, Sun Y, Di Costanzo N, Mitchell C, Achuthan A, Hamilton JA, Busuttil RA, Boussioutas A (2019) Macrophage spatial heterogeneity in gastric cancer defined by multiplex immunohistochemistry. Nat Commun 10:3928

Huber AL, Papp SJ, Chan AB, Henriksson E, Jordan SD, Kriebs A, Nguyen M, Wallace M, Li Z, Metallo CM et al (2016a) CRY2 and FBXL3 cooperatively degrade c-MYC. Mol Cell 64:774–789

Huber R, Meier B, Otsuka A, Fenini G, Satoh T, Gehrke S, Widmer D, Levesque MP, Mangana J, Kerl K et al (2016b) Tumour hypoxia promotes melanoma growth and metastasis via High Mobility Group Box-1 and M2-like macrophages. Sci Rep 6:29914

Hunt NH, Evans T (1980) RMI 12330A, an inhibitor of cyclic nucleotide phosphodiesterases and adenylate cyclase in kidney preparations. Biochim Biophys Acta 613:499–506

Jiang W, Le J, Wang P-y, Cheng X, Smelkinson M, Dong W, Yang C, Chu Y, Hwang PM, Munford RS et al (2021a) Extracellular acidity reprograms macrophage metabolism and innate responsiveness. GSE164697 [DATASET]

Jiang W, Le J, Wang P-y, Cheng X, Smelkinson M, Dong W, Yang C, Chu Y, Hwang PM, Munford RS et al (2021b) Extracellular Acidity Reprograms Macrophage Metabolism and Innate Responsiveness. J Immunol 206:3021–3031

Kato Y, Kawamoto T, Fujimoto K, Noshiro M (2014) Chapter Ten—DEC1/STRA13/SHARP2 and DEC2/SHARP1 coordinate physiological processes, including circadian rhythms in response to environmental stimuli. In: Taneja R (ed.) Current topics in developmental biology. Academic Press, pp 339–372

Keller M, Mazuch J, Abraham U, Eom GD, Herzog ED, Volk HD, Kramer A, Maier B (2009) A circadian clock in macrophages controls inflammatory immune responses. Proc Natl Acad Sci USA 106:21407–21412

Keller M, Mazuch J, Abraham U, Eom GD, Herzog ED, Volk HD, Kramer A, Maier B (2010) Circadian transcriptional profiling of peritoneal macrophages. GSE25585 [DATASET]

Kidiyoor A, Schettini J, Besmer DM, Rego SL, Nath S, Curry JM, Roy LD, Dreau D, Mukherjee P (2014) Pancreatic cancer cells isolated from Muc1-Null tumors favor the generation of a mature less suppressive MDSC population. Front Immunol 5:67

Kitchen GB, Cunningham PS, Poolman TM, Iqbal M, Maidstone R, Baxter M, Bagnall J, Begley N, Saer B, Hussell T et al (2019) The clock gene BMAL1 inhibits macrophage motility, phagocytosis, and impairs defence against pneumonia. E-MTAB-8411 [DATASET]

Kitchen GB, Cunningham PS, Poolman TM, Iqbal M, Maidstone R, Baxter M, Bagnall J, Begley N, Saer B, Hussell T et al (2020) The clock gene Bmal1 inhibits macrophage motility, phagocytosis, and impairs defense against pneumonia. Proc Natl Acad Sci USA 117(3):1543–1551

Kraut JA, Madias NE (2014) Lactic acidosis. N. Engl J Med 371:2309–2319

Kuang DM, Zhao Q, Peng C, Xu J, Zhang JP, Wu C, Zheng L (2009) Activated monocytes in peritumoral stroma of hepatocellular carcinoma foster immune privilege and disease progression through PD-L1. J Exp Med 206:1327–1337

Lavin Y, Kobayashi S, Leader A, Amir ED, Elefant N, Bigenwald C, Remark R, Sweeney R, Becker CD, Levine JH et al (2017) Innate immune landscape in early lung adenocarcinoma by paired single-cell analyses. Cell 169:750–765.e717

Laviron M, Petit M, Weber-Delacroix E, Combes AJ, Arkal AR, Barthélémy S, Courau T, Hume DA, Combadière C, Krummel MF et al (2022) Tumor-associated macrophage heterogeneity is driven by tissue territories in breast cancer. Cell Rep 39:110865

Layoun A, Samba M, Santos MM (2015) Isolation of murine peritoneal macrophages to carry out gene expression analysis upon Toll-like receptors stimulation. J Vis Exp e52749 https://doi.org/10.3791/52749

Lee C-C, Lin J-C, Hwang W-L, Kuo Y-J, Chen H-K, Tai S-K, Lin C-C, Yang M-H (2018) Macrophage-secreted interleukin-35 regulates cancer cell plasticity to facilitate metastatic colonization. Nat Commun 9:3763

Lellupitiyage Don SS, Mas-Rosario JA, Lin HH, Nguyen EM, Taylor SR, Farkas ME (2022) Macrophage circadian rhythms are differentially affected based on stimuli. Integr Biol 14:62–75

Liu C, Li S, Liu T, Borjigin J, Lin JD (2007) Transcriptional coactivator PGC-1alpha integrates the mammalian clock and energy metabolism. Nature 447:477–481

Liu PS, Wang H, Li X, Chao T, Teav T, Christen S, Di Conza G, Cheng WC, Chou CH, Vavakova M et al (2017) alpha-ketoglutarate orchestrates macrophage activation through metabolic and epigenetic reprogramming. Nat Immunol 18:985–994

Long JE, Drayson MT, Taylor AE, Toellner KM, Lord JM, Phillips AC (2016) Morning vaccination enhances antibody response over afternoon vaccination: a cluster-randomised trial. Vaccine 34:2679–2685

Lv S, Li J, Qiu X, Li W, Zhang C, Zhang ZN, Luan B (2017) A negative feedback loop of ICER and NF-κB regulates TLR signaling in innate immune responses. Cell Death Differ 24:492–499

Lyssiotis CA, Kimmelman AC (2017) Metabolic interactions in the tumor microenvironment. Trends Cell Biol 27:863–875

Mantovani A, Allavena P, Marchesi F, Garlanda C (2022) Macrophages as tools and targets in cancer therapy. Nat Rev Drug Discov 21:799–820

Mantovani A, Biswas SK, Galdiero MR, Sica A, Locati M (2013) Macrophage plasticity and polarization in tissue repair and remodelling. J Pathol 229:176–185

Martinez FO, Gordon S (2014) The M1 and M2 paradigm of macrophage activation: time for reassessment. F1000prime Rep. 6:13

Massagué J (2008) TGFb in cancer. Cell 134:215–230

Mazzoccoli G, Sothern RB, De Cata A, Giuliani F, Fontana A, Copetti M, Pellegrini F, Tarquini R (2011) A timetable of 24-hour patterns for human lymphocyte subpopulations. J Biol Regul Homeost Agents 25:387–395

McWhorter FY, Wang T, Nguyen P, Chung T, Liu WF (2013) Modulation of macrophage phenotype by cell shape. Proc Natl Acad Sci USA 110:17253–17258

Mills BN, Connolly KA, Ye J, Murphy JD, Uccello TP, Han BJ, Zhao T, Drage MG, Murthy A, Qiu H et al (2019) Stereotactic body radiation and interleukin-12 combination therapy eradicates pancreatic tumors by repolarizing the immune microenvironment. Cell Rep 29:406–421.e405

Mills CD, Kincaid K, Alt JM, Heilman MJ, Hill AM (2000) M-1/M-2 macrophages and the Th1/Th2 paradigm. J Immunol 164:6166–6173

Misra UK, Pizzo SV (2005) Coordinate regulation of forskolin-induced cellular proliferation in macrophages by protein kinase A/cAMP-response element-binding protein (CREB) and Epac1-Rap1 signaling: effects of silencing CREB gene expression on Akt activation. J Biol Chem 280:38276–38289

Mosser DM, Edwards JP (2008) Exploring the full spectrum of macrophage activation. Nat Rev Immunol 8:958–969

Munder M, Eichmann K, Modolell M (1998) Alternative metabolic states in murine macrophages reflected by the nitric oxide synthase/arginase balance: competitive regulation by CD4+ T cells correlates with Th1/Th2 phenotype. J Immunol 160:5347–5354

Mure LS, Le HD, Benegiamo G, Chang MW, Rios L, Jillani N, Ngotho M, Kariuki T, Dkhissi-Benyahya O, Cooper HM et al (2018) Diurnal transcriptome atlas of a primate across major neural and peripheral tissues. Science 359:eaao0318

Murray PJ (2017) Macrophage polarization. Annu Rev Physiol 79:541–566

Murray PJ (2018) Nonresolving macrophage-mediated inflammation in malignancy. FEBS J 285:641–653

Murray PJ, Wynn TA (2011) Protective and pathogenic functions of macrophage subsets. Nat Rev Immunol 11:723–737

Nalio Ramos R, Missolo-Koussou Y, Gerber-Ferder Y, Bromley CP, Bugatti M, Núñez NG, Tosello Boari J, Richer W, Menger L, Denizeau J et al (2022) Tissue-resident FOLR2(+) macrophages associate with CD8(+) T cell infiltration in human breast cancer. Cell 185:1189–1207.e1125

Nathan CF, Murray HW, Wiebe ME, Rubin BY (1983) Identification of interferon-gamma as the lymphokine that activates human macrophage oxidative metabolism and antimicrobial activity. J Exp Med 158:670–689

Nguyen KD, Fentress SJ, Qiu Y, Yun K, Cox JS, Chawla A (2013) Circadian gene Bmal1 regulates diurnal oscillations of Ly6C(hi) inflammatory monocytes. Science 341:1483–1488

Ni L, Fang P, Hu ZL, Zhou HY, Chen JG, Wang F, Jin Y (2018) Identification and function of acid-sensing ion channels in RAW 264.7 macrophage cells. Curr Med Sci 38:436–442

Nobis CC, Dubeau Laramée G, Kervezee L, Maurice De Sousa D, Labrecque N, Cermakian N (2019) The circadian clock of CD8 T cells modulates their early response to vaccination and the rhythmicity of related signaling pathways. Proc Natl Acad Sci USA 116:20077–20086

Odegaard JI, Ricardo-Gonzalez RR, Goforth MH, Morel CR, Subramanian V, Mukundan L, Eagle AR, Vats D, Brombacher F, Ferrante AW et al (2007)

Macrophage-specific PPARγ controls alternative activation and improves insulin resistance. Nature 447:1116–1120

O'Neill JS, Maywood ES, Chesham JE, Takahashi JS, Hastings MH (2008) cAMP-dependent signaling as a core component of the mammalian circadian pacemaker. Science 320:949–953

O'Neill JS, Reddy AB (2012) The essential role of cAMP/Ca2+ signalling in mammalian circadian timekeeping. Biochem Soc Trans 40:44–50

Pariollaud M, Ibrahim LH, Irizarry E, Mello RM, Chan AB, Altman BJ, Shaw RJ, Bollong MJ, Wiseman RL, Lamia KA (2022) Circadian disruption enhances HSF1 signaling and tumorigenesis in Kras-driven lung cancer. Sci Adv 8:eabo1123

Partch CL, Green CB, Takahashi JS (2014) Molecular architecture of the mammalian circadian clock. Trends Cell Biol 24:90–99

Pastore N, Brady OA, Diab HI, Martina JA, Sun L, Huynh T, Lim JA, Zare H, Raben N, Ballabio A et al (2016) TFEB and TFE3 cooperate in the regulation of the innate immune response in activated macrophages. Autophagy 12:1240–1258

Pastorekova S, Gillies RJ (2019) The role of carbonic anhydrase IX in cancer development: links to hypoxia, acidosis, and beyond. Cancer Metastasis Rev 38:65–77

Patro R, Duggal G, Love MI, Irizarry RA, Kingsford C (2017) Salmon provides fast and bias-aware quantification of transcript expression. Nat Methods 14:417–419

Pello OM, De Pizzol M, Mirolo M, Soucek L, Zammataro L, Amabile A, Doni A, Nebuloni M, Swigart LB, Evan GI et al (2012) Role of c-MYC in alternative activation of human macrophages and tumor-associated macrophage biology. Blood 119:411–421

Pesce JT, Ramalingam TR, Wilson MS, Mentink-Kane MM, Thompson RW, Cheever AW, Urban JF Jr, Wynn TA (2009) Retnla (relmalpha/fizz1) suppresses helminth-induced Th2-type immunity. PLoS Pathog 5:e1000393

Phillips AC, Gallagher S, Carroll D, Drayson M (2008) Preliminary evidence that morning vaccination is associated with an enhanced antibody response in men. Psychophysiology 45:663–666

Pilorz V, Cunningham PS, Jackson A, West AC, Wager TT, Loudon ASI, Bechtold DA (2014) A novel mechanism controlling resetting speed of the circadian clock to environmental stimuli. Curr Biol 24:766–773

Polumuri S, Perkins DJ, Vogel SN (2021) cAMP levels regulate macrophage alternative activation marker expression. Innate Immun 27:133–142

Qian DC, Kleber T, Brammer B, Xu KM, Switchenko JM, Janopaul-Naylor JR, Zhong J, Yushak ML, Harvey RD, Paulos CM et al (2021) Effect of immunotherapy time-of-day infusion on overall survival among patients with advanced melanoma in the USA (MEMOIR): a propensity score-matched analysis of a single-centre, longitudinal study. Lancet Oncol 22:1777–1786

Raghunand N, Gatenby RA, Gillies RJ (2003) Microenvironmental and cellular consequences of altered blood flow in tumours. Br J Radio 76:S11–22

Ramanathan C, Xu H, Khan SK, Shen Y, Gitis PJ, Welsh DK, Hogenesch JB, Liu AC (2014) Cell type-specific functions of period genes revealed by novel adipocyte and hepatocyte circadian clock models. PLOS Genet 10:e1004244

Ray A, Dittel BN (2010) Isolation of mouse peritoneal cavity cells. J Vis Exp 35:e1488

Rehli M, Sulzbacher S, Pape S, Ravasi T, Wells CA, Heinz S, Söllner L, El Chartouni C, Krause SW, Steingrimsson E et al (2005) Transcription factor Tfec contributes to the IL-4-inducible expression of a small group of genes in mouse macrophages including the granulocyte colony-stimulating factor receptor. J Immunol 174:7111–7122

Ritchie ME, Phipson B, Wu D, Hu Y, Law CW, Shi W, Smyth GK (2015) limma powers differential expression analyses for RNA-sequencing and microarray studies. Nucleic Acids Res 43:e47

Roberts AW, Lee BL, Deguine J, John S, Shlomchik MJ, Barton GM (2017) Tissue-resident macrophages are locally programmed for silent clearance of apoptotic cells. Immunity 47:913–927.e916

Rodheim K, Jung C, Wright K (2021) 016 Associations between circadian melatonin and temperature amplitudes during constant routine. Sleep 44:A8–A8

Ruffell B, Coussens LM (2015) Macrophages and therapeutic resistance in cancer. Cancer Cell 27:462–472

Sato S, Sakurai T, Ogasawara J, Takahashi M, Izawa T, Imaizumi K, Taniguchi N, Ohno H, Kizaki T (2014) A circadian clock gene, Rev-erbalpha, modulates the inflammatory function of macrophages through the negative regulation of Ccl2 expression. J Immunol 192:407–417

Scheiermann C, Gibbs J, Ince L, Loudon A (2018) Clocking in to immunity. Nat Rev Immunol 18:423–437

Schoppmann SF, Birner P, Stöckl J, Kalt R, Ullrich R, Caucig C, Kriehuber E, Nagy K, Alitalo K, Kerjaschki D (2002) Tumor-associated macrophages express lymphatic endothelial growth factors and are related to peritumoral lymphangiogenesis. Am J Pathol 161:947–956

Selezneva A, Gibb AJ, Willis D (2022) The contribution of ion channels to shaping macrophage behaviour. Front Pharm 13:970234

Shaykhiev R, Krause A, Salit J, Strulovici-Barel Y, Harvey BG, O'Connor TP, Crystal RG (2009a) Smoking-dependent reprogramming of alveolar macrophage polarization: implication for pathogenesis of chronic obstructive pulmonary disease. J Immunol 183:2867–2883

Shaykhiev R, Krause A, Salit J, Strulovici-Barel Y, Harvey BG, O'Connor TP, Crystal RG (2009b) Smoking-dependent reprogramming of alveolar macrophage polarization: implication for pathogenesis of COPD. GSE13896 [DATASET]

Shilts J, Chen G, Hughey JJ (2018) Evidence for widespread dysregulation of circadian clock progression in human cancer. PeerJ 6:e4327

Silver AC, Arjona A, Hughes ME, Nitabach MN, Fikrig E (2012a) Circadian expression of clock genes in mouse macrophages, dendritic cells, and B cells. Brain Behav Immun 26:407–413

Silver AC, Arjona A, Walker WE, Fikrig E (2012b) The circadian clock controls toll-like receptor 9-mediated innate and adaptive immunity. Immunity 36:251–261

Smyth GK (2005) limma: linear models for microarray data. In: Gentleman R, Carey VJ, Huber W, Irizarry RA, Dudoit S (eds) Bioinformatics and computational biology solutions using R and bioconductor. Springer New York, New York, pp 397–420

Soneson C, Love MI, Robinson MD (2015) Differential analyses for RNA-seq: transcript-level estimates improve gene-level inferences. F1000Res 4:1521

Stein M, Keshav S, Harris N, Gordon S (1992) Interleukin 4 potently enhances murine macrophage mannose receptor activity: a marker of alternative immunologic macrophage activation. J Exp Med 176:287–292

Storch KF, Paz C, Signorovitch J, Raviola E, Pawlyk B, Li T, Weitz CJ (2007) Intrinsic circadian clock of the mammalian retina: importance for retinal processing of visual information. Cell 130:730–741

Storrs EP, Chati P, Usmani A, Sloan I, Krasnick BA, Babbra R, Harris PK, Sachs CM, Qaium F, Chatterjee D et al (2023) High-dimensional deconstruction of pancreatic cancer identifies tumor microenvironmental and developmental stemness features that predict survival. NPJ Precis Oncol 7:105

Strassmann G, Patil-Koota V, Finkelman F, Fong M, Kambayashi T (1994) Evidence for the involvement of interleukin 10 in the differential deactivation of murine peritoneal macrophages by prostaglandin E2. J Exp Med 180:2365–2370

Strauss L, Mahmoud MAA, Weaver JD, Tijaro-Ovalle NM, Christofides A, Wang Q, Pal R, Yuan M, Asara J, Patsoukis N et al (2020) Targeted deletion of PD-1 in myeloid cells induces antitumor immunity. Sci Immunol 5:eaay1863

Swietach P (2019) What is pH regulation, and why do cancer cells need it? Cancer Metastasis Rev 38:5–15

Takahashi JS (2017) Transcriptional architecture of the mammalian circadian clock. Nat Rev Genet 18:164–179

Tavares LP, Negreiros-Lima GL, Lima KM, PMR ES, Pinho V, Teixeira MM, Sousa LP (2020) Blame the signaling: role of cAMP for the resolution of inflammation. Pharm Res 159:105030

Tomayko MM, Reynolds CP (1989) Determination of subcutaneous tumor size in athymic (nude) mice. Cancer Chemother Pharm 24:148–154

Trouplin V, Boucherit N, Gorvel L, Conti F, Mottola G, Ghigo E (2013) Bone marrow-derived macrophage production. J Vis Exp e50966 https://doi.org/10.3791/50966

Tsuruta A, Shiiba Y, Matsunaga N, Fujimoto M, Yoshida Y, Koyanagi S, Ohdo S (2022) Diurnal expression of PD-1 on tumor-associated macrophages underlies the dosing time-dependent antitumor effects of the PD-1/PD-L1 inhibitor BMS-1 in B16/BL6 melanoma-bearing mice. Mol Cancer Res 20:972–982

van Rossum DB, Patterson RL, Ma HT, Gill DL (2000) Ca^{2+} entry mediated by store depletion, S-nitrosylation, and TRP3 channels. Comparison of coupling and function. J Biol Chem 275:28562–28568

Viola A, Munari F, Sánchez-Rodríguez R, Scolaro T, Castegna A (2019) The metabolic signature of macrophage responses. Front Immunol 10:1462

Walton ZE, Brooks RC, Dang CV (2019) mTOR senses intracellular pH through lysosome dispersion from RHEB. BioEssays 41:e1800265

Walton ZE, Patel CH, Brooks RC, Yu Y, Ibrahim-Hashim A, Riddle M, Porcu A, Jiang T, Ecker BL, Tameire F et al (2018) Acid suspends the circadian clock in hypoxia through inhibition of mTOR. Cell 174:72–87.e32

Wang C, Zeng Q, Gül ZM, Wang S, Pick R, Cheng P, Bill R, Wu Y, Naulaerts S, Barnoud C et al (2024a) Circadian tumor infiltration and function of CD8+ T cells dictate a temporal response to immunotherapy. GSE260641 [DATASET]

Wang C, Zeng Q, Gül ZM, Wang S, Pick R, Cheng P, Bill R, Wu Y, Naulaerts S, Barnoud C et al (2024b) Circadian tumor infiltration and function of CD8+ T cells dictate immunotherapy efficacy. Cell 187:2690–2702.e2617

Wu G, Francey LJ, Ruben MD, Hogenesch JB (2021) Normalized coefficient of variation (nCV): a method to evaluate circadian clock robustness in population scale data. Bioinformatics 37:4581–4583

Yagita K, Okamura H (2000) Forskolin induces circadian gene expression of rPer1, rPer2 and dbp in mammalian rat-1 fibroblasts. FEBS Lett 465:79–82

Yano S, Zhang Y, Miwa S, Tome Y, Hiroshima Y, Uehara F, Yamamoto M, Suetsugu A, Kishimoto H, Tazawa H et al (2014) Spatial-temporal FUCCI imaging of each cell in a tumor demonstrates locational dependence of cell cycle dynamics and chemoresponsiveness. Cell Cycle 13:2110–2119

Yoo SH, Yamazaki S, Lowrey PL, Shimomura K, Ko CH, Buhr ED, Siepka SM, Hong HK, Oh WJ, Yoo OJ et al (2004) PERIOD2::LUCIFERASE real-time reporting of circadian dynamics reveals persistent circadian oscillations in mouse peripheral tissues. Proc Natl Acad Sci USA 101:5339–5346

Zhang QW, Liu L, Gong CY, Shi HS, Zeng YH, Wang XZ, Zhao YW, Wei YQ (2012) Prognostic significance of tumor-associated macrophages in solid tumor: a meta-analysis of the literature. PLoS ONE 7:e50946

Zhang R, Lahens NF, Ballance HI, Hughes ME, Hogenesch JB (2014) A circadian gene expression atlas in mammals: implications for biology and medicine. Proc Natl Acad Sci USA 111:16219–16224

Acknowledgements

Author contributions

Disclosure and competing interests statement
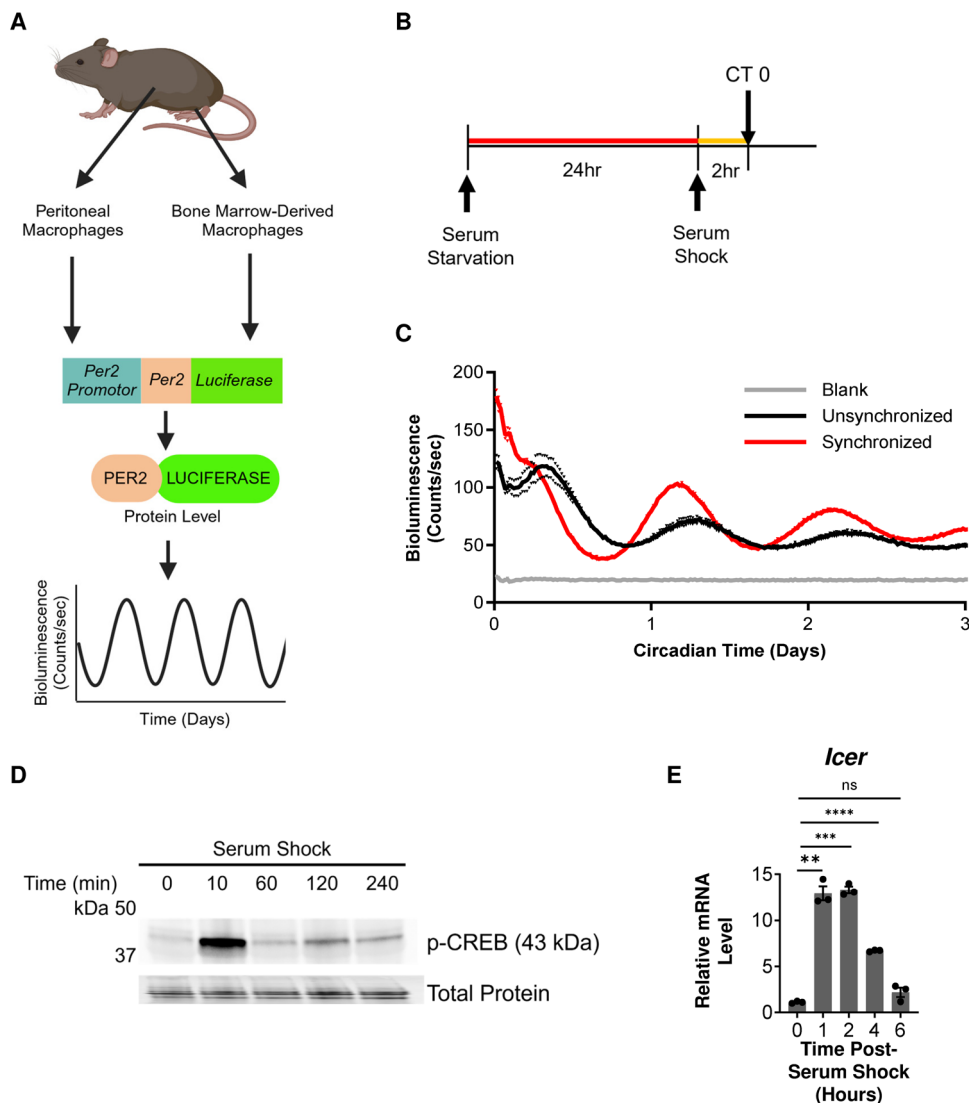
Expanded View Figures

Figure EV1. The PER2-Luciferase reporter system enables real-time monitoring of circadian rhythms of macrophages.

(A) A schematic of the Per2-Luciferase (Per2-Luc) luciferase reporter system. (B) A schematic of the synchronization protocol in which the circadian clocks of bone marrow-derived macrophages (BMDMs) derived from C57BL/6 mice expressing Per2-Luc were synchronized by a 24-h period of serum starvation in media with 0% serum, followed by a 2-h period of serum shock in media with 50% serum. (C) BMDMs were then cultured in RPMI/10% FBS supplemented with D-luciferin at circadian time (CT) 0. Luciferase activity of BMDMs was monitored in real time by LumiCycle, $n = 2$ biological replicates. (D, E) Protein and RNA were collected at the indicated times post-serum shock to assess (D) cAMP signaling by p-CREB levels and (E) expression of *Icer*, $n = 3$ biological replicates. Data information: For (C–E), experiments were replicated twice. For (C), shown are individual points and mean. For (E), mean and SEM are shown, and statistical significance determined by unpaired two-tailed t-test with Welch's correction; *$p < 0.05$; **$p < 0.005$; ***$p < 0.0005$; ****$p < 0.0001$; ns: not significant. Exact p values: (E) 0.0039 (0 h vs 1 h), 0.0006 (0 h vs 2 h), <0.0001 (0 h vs 4 h).
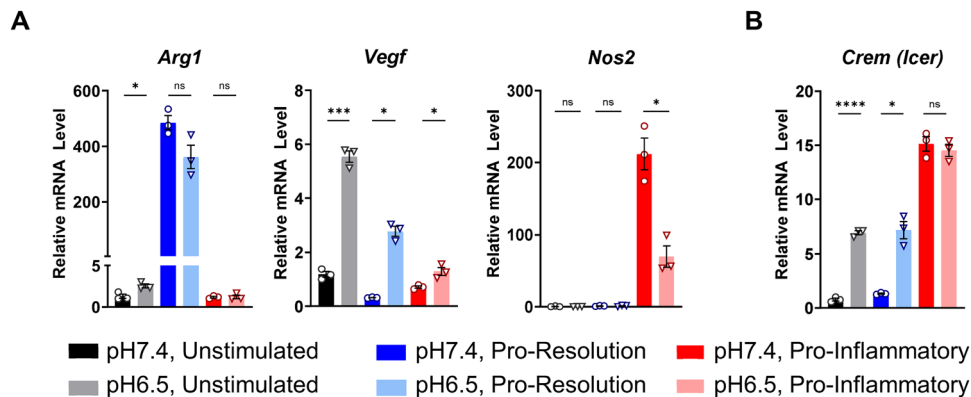
Figure EV2. Macrophages sense and respond to an acidic extracellular environment when cultured in vitro in media with acidic pH.

(A, B) Bone marrow-derived macrophages (BMDMs) were obtained from C57BL/6 mice expressing PER2-Luc. BMDMs were cultured in media with pH 7.4 or acidic media with pH 6.5, and stimulated with either 10 ng/mL IL-4 and 10 ng/mL IL-13 (pro-resolution), or 50 ng/mL IFNγ and 100 ng/mL LPS (pro-inflammatory); or left unstimulated. RNA was collected at 2 h post-treatment, and qt-PCR was performed to assess expression of genes associated with (A) phenotype or (B) acid sensing in macrophages. For both panels, $n = 3$ biological replicates. Data information: Shown are mean and SEM. Statistical significance determined by two-tailed t-test with Welch's correction. The Holm-Šídák correction for multiple t-tests were applied; $*p < 0.05$; $**p < 0.005$; $***p < 0.0005$; $****p < 0.0001$; ns: not significant. Experiments were replicated twice. Exact p values: (A) *Arg1* 0.024372 (pH 7.4 vs pH 6.5 unstimulated); *Vegf* 0.000403 (pH 7.4 vs pH 6.5 unstimulated), 0.011077 (pH 7.4 vs pH 6.5 pro-resolution), 0.048413 (pH 7.4 vs pH 6.5 pro-Inflammatory); *Nos2* 0.008509 (pH 7.4 vs pH 6.5 pro-inflammatory). (B) *Icer* < 0.0001 (pH 7.4 vs pH 6.5 unstimulated), 0.01749 (pH 7.4 vs pH 6.5 pro-resolution).
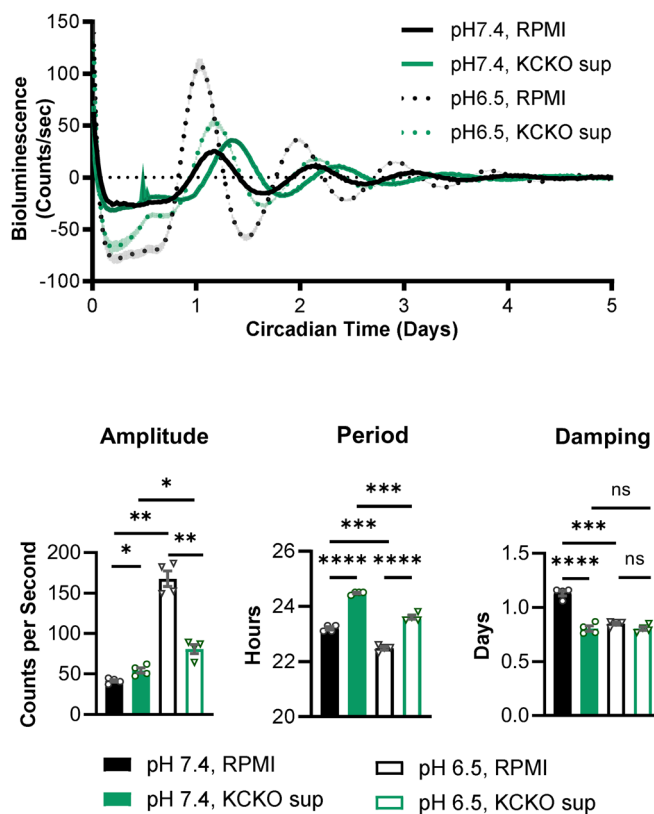
Figure EV3. **Exposure to cancer cell supernatant further modulates circadian rhythms in addition to pH-driven changes.**

Bone marrow-derived macrophages (BMDMs) were obtained from C57BL/6 mice expressing Per2-Luc. The circadian clocks of BMDMs were synchronized by a 24-h period of serum starvation in media with 0% serum, followed by a 2-h period of serum shock in media with 50% serum. BMDMs were then cultured in RPMI with neutral pH 7.4 or acidic pH 6.5, or in KCKO supernatant at pH 6.5 or pH-adjusted to pH 7.4. Luciferase activity was monitored in real time by LumiCycle. Data was baseline-subtracted using the running average, and oscillation parameters were measured by LumiCycle Analysis, $n = 4$ biological replicates. Data information: Shown is the mean and SEM. Statistical significance determined by unpaired two-tailed t-test with Welch's correction; *$p < 0.05$; **$p < 0.005$; ***$p < 0.0005$; ****$p < 0.0001$; ns: not significant. Exact p values: Amplitude 0.0216 (pH 7.4 RPMI vs pH 7.4 KCKO sup), 0.0008 (pH 7.4 RPMI vs pH 6.5 RPMI), 0.0105 (pH 7.4 KCKO sup vs pH 6.5 KCKO sup), 0.0007 (pH 6.5 RPMI vs pH 6.5 KCKO sup); Period <0.0001 (pH 7.4 RPMI vs pH 7.4 KCKO sup), 0.0002 (pH 7.4 RPMI vs pH 6.5 RPMI), 0.0004 (pH 7.4 KCKO sup vs pH 6.5 KCKO sup), <0.0001 (pH 6.5 RPMI vs pH 6.5 KCKO sup); Damping <0.0001 (pH 7.4 RPMI vs pH 7.4 KCKO sup), 0.0002 (pH 7.4 RPMI vs pH 6.5 RPMI).
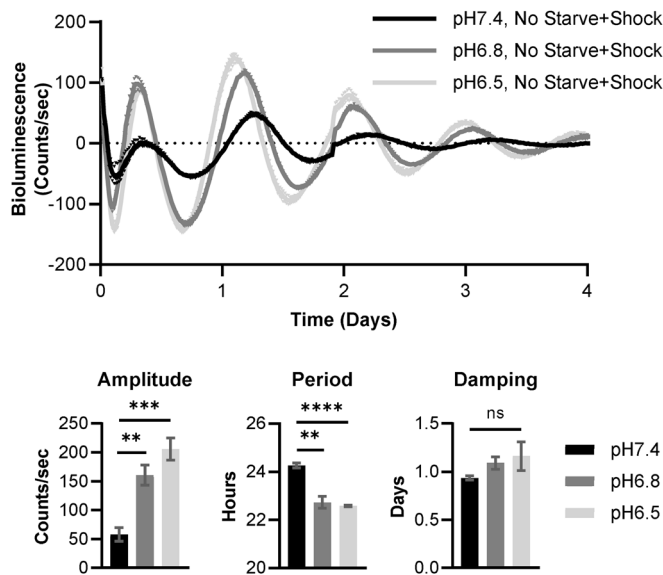
Figure EV4. Acidic pH alters circadian rhythms in macrophages in the absence of prior serum starvation followed by serum shock.

Bone marrow-derived macrophages (BMDMs) were obtained from C57BL/6 mice expressing Per2-Luc. BMDMs were cultured in media with neutral pH 7.4 or acidic pH 6.8 or 6.5. Luciferase activity was monitored in real time by LumiCycle (pH 7.4: $n = 3$. pH 6.8: $n = 2$. pH 6.5: $n = 3$). Data was baseline-subtracted using the running average, and oscillation parameters were measured by LumiCycle Analysis (pH 7.4: $n = 5$. pH 6.8: $n = 4$. pH 6.5: $n = 5$, data pooled from 2 individual experiments). Data information: For LumiCycle traces, shown are individual points and mean. For LumiCycle analysis, shown is the mean and SEM. Statistical significance determined by unpaired two-tailed t-test with Welch's correction (pH 6.8 and 6.5 comparison not tested); **$p < 0.005$; ***$p < 0.0005$; ****$p < 0.0001$. Exact p values: Amplitude 0.0035 (pH 7.4 vs pH 6.8), 0.0004 (pH 7.4 vs pH 6.5); Period 0.0044 (pH 7.4 vs pH 6.8), <0.0001 (pH 7.4 vs pH 6.5).
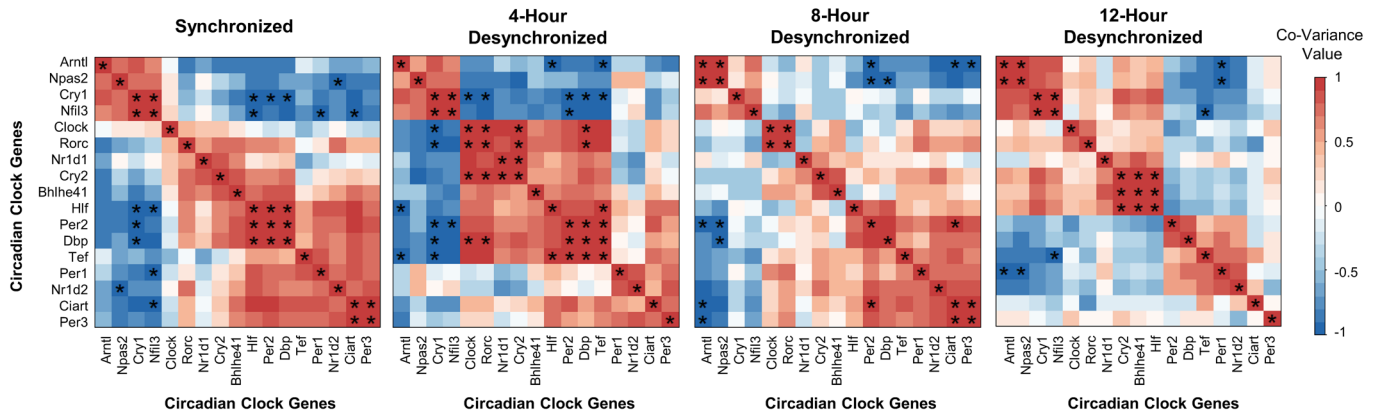
Figure EV5. Heterogeneity in circadian rhythms of cells within a population can lead to an altered circadian clock gene network in samples.

Increasingly desynchronized populations were modeled using an RNA-seq data set of WT peritoneal macrophages taken at 4-h intervals across two days, $n = 12$ biological replicates (see Fig. 8 and Methods). Weighted gene co-expression network analysis (WGCNA) was performed. Data information: *$p < 0.01$ by WGCNA for significant covariance by Pearson correlation, and blank squares are not significant.